



Published in final edited form as:

J Med Chem. 2018 June 14; 61(11): 4739–4756. doi:10.1021/acs.jmedchem.7b01839.

Expanding benzoxazole based inosine 5'-monophosphate dehydrogenase (IMPDH) inhibitor structure-activity as potential anti-tuberculosis agents

Shibin Chacko[§], Helena I. M. Boshoff[#], Vinayak Singh[†], Davide M. Ferraris^{‡‡}, Deviprasad R. Gollapalli[§], Minjia Zhang[§], Ann P. Lawson[§], Michael J. Pepi^{¶¶}, Andrzej Joachimiak[‡], Menico Rizzi^{‡‡}, Valerie Mizrahi[†], Gregory D. Cuny^{*‡}, and Lizbeth Hedstrom^{*§¶}

[§]Department of Biology Brandeis University, 415 South St. Waltham, Massachusetts 02454, United States

^{¶¶}Department of Chemistry, Brandeis University, 415 South St. Waltham, Massachusetts 02454, United States

[#]Tuberculosis Research Section, National Institute of Allergy and Infectious Diseases, Bethesda, Maryland 20892, United States

[†]MRC/NHLS/UCT Molecular Mycobacteriology Research Unit & DST/NRF Centre of Excellence for Biomedical TB Research, Institute of Infectious Disease and Molecular Medicine & Department of Pathology, University of Cape Town, Anzio Road, Observatory 7925, South Africa

[‡]Center for Structural Genomics of Infectious Diseases, University of Chicago, Chicago, IL 60557 and Structural Biology Center, Biosciences, Argonne National Laboratory, 9700 S Cass Ave. Argonne, IL 60439, USA

^{‡‡}Dipartimento di Scienze del Farmaco, University of Piemonte Orientale, Via Bovio 6, 28100 Novara, Italy

[‡]Department of Pharmacological and Pharmaceutical Sciences, College of Pharmacy, University of Houston, Health Building 2, 4849 Calhoun Rd., Houston, Texas 77204, United States

Abstract

New drugs and molecular targets are urgently needed to address the emergence and spread of drug-resistant tuberculosis. *Mycobacterium tuberculosis* (*Mtb*) inosine 5'-monophosphate dehydrogenase 2 (*Mtb*IMPDH2) is a promising yet controversial potential target. Inhibition of *Mtb*IMPDH2 blocks the biosynthesis of guanine nucleotides, but high concentrations of guanine can potentially rescue the bacteria. Herein we describe an expansion of the structure-activity relationship (SAR) for the benzoxazole series of *Mtb*IMPDH2 inhibitors and demonstrate that minimum inhibitory concentrations (MIC) of 1 μ M can be achieved. The antibacterial activity of

*Corresponding Authors: gdcuny@central.uh.edu, Tel no.: 1-713-743-1274. hedstrom@brandeis.edu, Tel no.: 1-781-736-2333.

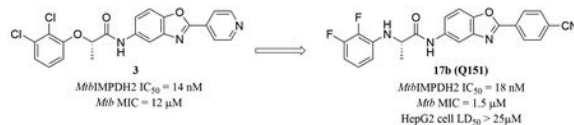
Present addresses: Shibin Chacko, University of Kansas, Synthetic Chemical Biology Core Facility, Structural Biology Center, 2034 Becker Drive, Lawrence, KS 66047–1620.

Vinayak Singh, H3D Drug Discovery and Development Centre, Department of Drug Discovery and Development & Institute of Infectious Disease and Molecular Medicine, University of Cape Town, Rondebosch 7701, Cape Town, South Africa

Supporting Information: CSV file with molecular formula strings and the associated biochemical and biological data.

the most promising compound, **17b (Q151)**, derives from inhibition of *Mtb*IMPDH2 as demonstrated by conditional knockdown and resistant strains. Importantly, guanine does not change the MIC of **17b**, alleviating the concern that guanine salvage can protect *Mtb* *in vivo*. These findings suggest that *Mtb*IMPDH2 is a vulnerable target for tuberculosis.

Table of Content graphic



INTRODUCTION

The worldwide burden of tuberculosis is staggering: more than 1 million deaths and 10 million new cases occur each year (<https://www.cdc.gov/tb/statistics/default.htm>, accessed 5/21/2017). Approximately one third of the world's population is infected with the causative agent *Mycobacterium tuberculosis* (*Mtb*), many with latent infections that can recrudesce if the patient becomes immunosuppressed. Treatment requires administration with isoniazid, rifampicin pyrazinamide and ethambutol for two months followed by an additional four months with isoniazid and rifampicin. However, almost 0.5 million cases involve *Mtb* strains that are resistant to isoniazid and rifampicin, further complicating treatment. Extensively drug resistant strains have also emerged that are resistant to at least isoniazid and rifampicin, a fluoroquinolone, and any one of the second-line injectables, capreomycin, kanamycin and amikacin. Frustratingly, as illustrated by the newly approved tuberculosis drugs bedaquiline and delamanid¹, resistance can emerge just a few years after introduction of a new therapy, underscoring the critical need for new drugs, drug targets, and drug regimens to improve tuberculosis treatment and combat the relentless evolution of resistance.

Inosine 5'-monophosphate dehydrogenase (IMPDH) is the enzyme that catalyzes the NAD⁺-dependent conversion of inosine 5'-monophosphate (IMP) to xanthosine 5'-monophosphate (XMP). This reaction is the first and the rate limiting step in the *de novo* biosynthesis of guanine nucleotides and therefore controls the size of the guanine nucleotide pool.² IMPDH is an attractive target for the development of new antibiotics due to the essential role of guanine nucleotides in DNA and RNA synthesis, signal transduction, energy transfer, glycoprotein biosynthesis and many other processes involved in cell proliferation.³ *Mtb* has three genes, designated as *guaB1*, *guaB2* and *guaB3*, which encode IMPDH homologs. Only *guaB2* is essential,⁴⁻⁶ and only *guaB2* encodes an active IMPDH (*Mtb*IMPDH2).⁷ The proteins encoded by *guaB1* and *guaB3* are each missing key catalytic residues and neither display IMPDH activity⁷. The functions of these proteins are currently unknown.

*Mtb*IMPDH2 is a controversial target for tuberculosis. Several small molecule inhibitors of *Mtb*IMPDH2 have been identified that display antibacterial activity *in vitro* and in macrophages⁷⁻¹³, but as yet no compounds have been reported with activity in animal models of tuberculosis. Recently, Park et al. suggested that high levels of guanine (200–2000 μM¹⁰) in the lungs of infected rabbits and humans can protect bacteria from *Mtb*IMPDH2

inhibitors,¹⁰ calling into question the vulnerability of this target. However, the availability of free guanine for salvage is by no means certain since these concentrations exceed the solubility limit. More promisingly, Singh et al. constructed a conditional knockout of *guaB2* in *Mtb* and found that depletion of *Mtb*IMPDPH2 is rapidly bactericidal *in vitro*.¹¹ They also showed that silencing of *Mtb*IMPDPH2 expression prevented infection in mice¹¹, consistent with the lower levels of guanine found in mouse tissue (7–20 μM ¹⁰). On the basis of these findings, Singh et al. concluded that this enzyme is indeed vulnerable.¹¹

IMPDPH also appears to have moonlighting functions of unknown physiological consequence, which further complicates the question of whether it is a vulnerable target. The protein contains a regulatory CBS subdomain in addition to the catalytic (β/α)₈ domain. CBS domains bind nucleotides and modulate the activity of other enzymes and channels¹⁴. However, deletion of the CBS subdomain does not affect the activity of the catalytic domain in IMPDPH^{15–18}. The CBS subdomain binds ATP and/or GTP depending on the particular IMPDPH^{19–22}. These interactions modulate the oligomerization of tetramers to form octamers and higher order structures *in vitro*, with modest effects on enzymatic activity^{19–22}. The physiological relevance of ATP/GTP binding and these higher order structures is uncertain. Most interestingly, deletion of CBS subdomain dysregulates the purine nucleotide pools in *E. coli*, leading to the toxic accumulation of ATP and other adenine nucleotides^{23, 24}. IMPDPH binds nucleic acid and can act as a transcription factor in eukaryotes, and this activity is mediated by the CBS subdomain^{25–27}. IMPDPH also interacts with numerous other proteins in bacteria, including the ribosome, RNAP, amino acyl tRNA synthetases, penicillin binding proteins, uridylyate kinase, PRPP synthetase, adenylosuccinate synthetase and DNA helicase^{28, 29}. Neither the sites nor the physiological consequences of these interactions have been elucidated. Therefore it is possible that the essentiality of *guaB2* in *Mtb* derives from a moonlighting function rather than enzymatic activity. Moreover, the physiological consequences of enzyme inhibition may well be different from protein depletion, which downregulates both enzymatic and moonlighting activities³⁰. More potent *Mtb*IMPDPH2 inhibitors are required to resolve this conundrum and determine the vulnerability of *Mtb* infections to IMPDPH inhibition³¹.

We have developed triazole (**A**-series), benzimidazole (**C**-series), phthalazinone (**D**-series), 4-oxo-[1]benzopyrano[4,3-c]pyrazole (**N**-series), urea (**P**-series) and benzoxazole (**Q**-series) inhibitors of prokaryotic IMPDPHs, including *Mtb*IMPDPH2^{9, 32–40}. These inhibitors exploit the highly diverged cofactor binding site, which explains their selectivity for bacterial over eukaryotic orthologs of IMPDPH^{9, 17}. Individual members of the **A**, **D**, **P** and **Q**-series display antibacterial activity against *Mtb* as well as other pathogens^{9, 41, 42}. The best **Q** compound, **3** (Figure 1A), was a potent inhibitor of *Mtb*IMPDPH2 ($K_{i,app} = 14$ nM) and displayed moderate antibacterial activity (MIC = 6.3 and 11 μM in minimal GAST/Fe and rich 7H9/ADC/Tween media, respectively). The values of MIC increased 3 to 7-fold in the presence of guanine, suggesting that antibacterial activity resulted from the on-target inhibition of *Mtb*IMPDPH2.

Herein we report an expansion of the structure-activity relationship (SAR) for the **Q**-series of *Mtb*IMPDPH2 inhibitors and improved antibacterial activity. Importantly, antibacterial activity is not reduced in the presence of guanine for the most potent compounds.

Nonetheless, antibacterial activity appears to derive from the inhibition of *Mtb*IMPDH2 as demonstrated by conditional knockdown and resistant strains. These findings suggest that *Mtb*IMPDH2 is indeed a vulnerable target.

RESULTS AND DISCUSSION

Design strategy.

IMPDHs are a square planar homotetramers, with each monomer composed of two domains, the catalytic domain and a smaller domain containing tandem cystathione β -synthetase (CBS) motifs.⁴³ The physiological role of the CBS domain is unknown. Deletion of this domain does not impact enzymatic properties or tetramer formation, but does improve solubility and crystallization. The crystal structure of the CBS deletion variant of *Mtb*IMPDH2 (*Mtb*IMPDH2 CBS)⁹ in complex with IMP and inhibitor **3** reveals that the aromatic ring of the 2,3-dichloroaniline is involved in a π - π interaction with the purine base of IMP, whereas the amide participates in an ionic-dipole interaction of the NH with the carboxylate of Glu458 and a hydrogen bond of the amide carbonyl with a water molecule (Figure 1B). The nitrogen atom of the 1,3-benzoxazole interacts with a water molecule that also engages the main chain nitrogen and oxygen atoms of His286. Moreover, the 4-pyridyl-1,3-benzoxazole moiety of **3** binds in a hydrophobic pocket formed by Val60, Pro61, and Tyr487 and the pyridyl nitrogen atom interacts with the backbone carbonyl of Ser57 via a water network.⁹ This pocket is not present in human IMPDHs, explaining the selectivity of the compounds for bacterial IMPDHs. Note that the two sulfonamide inhibitors in Figure 1C do not extend into this pocket, perhaps explaining the higher affinity and selectivity of the **Q** compounds.^{10, 11}

Using this information, we explored several strategies to expand the SAR of the **Q**-series (Figure 2): (1) modifications to the pyridine or replacement of the 4-pyridyl with a phenyl containing various substituents that can interact (e.g. via hydrogen bonds and ionic-dipole interactions) with the side chain of Arg290; (2) modification of the 2,3-dichloroaniline with 2,3-difluorophenyl ethers to enhance cell permeability or phenyl ethers containing hydrophilic groups capable of forming interactions with IMP and Glu458; (3) modifications of the amide group via replacement with a thioamide or amine to further explore interactions with Glu458; (4) replacement of the benzoxazole with a imidazo[1,2-a]pyridine; (5) insertion of a methylene linker between the benzoxazole and phenyl that was used as a pyridine replacement. **Chemistry.** The synthesis used to generate ether linked **Q**-series derivatives is illustrated in Scheme 1. Arylbenzoxazoles **4** were directly synthesized by oxidative cyclization methods using 2-amino-4-nitrophenol and aldehydes in the presence of activated carbon (Darco KB) under an oxygen atmosphere. The nitro group was reduced using Pd/C under 1 atm hydrogen to give 5-amine-2-arylbenzoxazoles **5**. Enantiomerically pure phenyl ethers **6** were synthesized from (+)-methyl D-lactate and the corresponding phenol using Mitsunobu reaction conditions. The esters **6** were hydrolyzed to the corresponding acids **7**, and then coupled with various 5-amine-2-arylbenzoxazoles in the presence of EDC·HCl in DMF to yield **8**.³⁹ Furthermore, **8** (Ar = 4-OMePh, R = 2,3-diCl) was treated with Lawesson's reagent under standard conditions to generate thioamide **9** quantitatively. Ester **6a** was also treated with 1M DIBAL-H in DCM at -78 °C to generate

aldehyde **10**, which was subjected to reductive amination using **5** (Ar = 4-OMePh) and sodium triacetoxyborohydride in DCM to provide amine **11**.

The synthesis of an imidazo[1,2-a]pyridine analogue started by allowing 5-nitropyridin-2-amine to react with an α -bromoketone in the presence of NaHCO₃ in ethanol to give **12**. Nitro group reduction using SnCl₂ in ethanol followed by coupling with carboxylic acid **7** (R = 2,3-diCl) generated imidazo[1,2-a]pyridine **13**.

The synthesis of a derivative with a methylene linker between the benzoxazole and the benzene was undertaken. 2-Amino-4-nitrophenol was coupled with a 1,1-dibromoethylene derivative using DABCO in NMP at 100 °C to generate **14**. The nitro group was reduced using 10% Pd/C under a hydrogen atmosphere and the resulting amine was coupled with **7** (R = 2,3-diCl) using EDC·HCl in DMF to yield **15**.

Enantiopure *N*-arylated benzoxazole derivatives were synthesized using copper catalyzed Ullman type reactions. L-alanine was treated with aryl iodides in the presence of cesium carbonate and CuI in DMF for 24 h to provide the *N*-arylated amino acids **16a-b**.³⁹ Attempts to couple these materials with **5** (Ar = 4-CNPh) using EDC·HCl failed. However, using HATU as the coupling reagent in DMF resulted in formation of **17a-b**.

Scheme 2 depicts the functional group transformations to various substituents attached to the benzoxazole aryl group. Compounds **8i** and **8j** were subjected to alkylation reactions with ethyl 2-bromoacetate in the presence of K₂CO₃ and DMF to give **18a** and **18b**, respectively. These compounds were hydrolyzed using LiOH in THF:MeOH (1:3) to yield **19a** and **19b**, respectively. Carboxylic acid **19a** was also converted to ester **20** using propargyl bromide and K₂CO₃ in dry DMF. Ester **8h** was also converted to an array of derivatives. For example, it was treated with hydroxylamine hydrochloride to provide the corresponding hydroxamic acid **21**. Base catalyzed ester hydrolysis of **8h** in MeOH:THF:H₂O (3:1:1) yielded carboxylic acid **22**. Finally, ester **8h** was converted to hydrazide **23** using hydrazine hydrate in EtOH, followed by treatment with carbonyl diimidazole (CDI) in the presence of DIPEA in DMF yielding 1,3,4-oxadiazolone **24**.

Scheme 3 illustrates the synthesis of an array of derivatives via functional group transformation of **8f**. For example, **8f** was treated with hydroxylamine hydrochloride in absolute ethanol in the presence of triethylamine to afford hydroxamidine **25**, which upon treatment with CDI and DIPEA gave 1,2,4-oxadiazolone **26**. The tetrazole derivative **27** was prepared by treatment of **8f** with sodium azide in the presence of ammonium chloride in dry DMF. Primary amide **28** was generated by treating **8f** with *t*-BuOK in *t*-BuOH.⁴⁵ Finally, **8f** was treated with NiCl₂·6H₂O and NaBH₄ in the presence of Boc₂O in MeOH:THF to give the Boc protected primary amine, which was deprotected using trifluoroacetic acid in DCM to provide **29**.⁴⁶

The synthesis of 2-pyridone derivative **30** was carried out by treating **8b** with LiCl and *p*-toluenesulfonic acid in anhydrous methanol (Scheme 4). The pyridyl of **8a** was oxidized using *m*-CPBA in DCM to give the corresponding pyridine N-oxide **31**. The nitrile in **8u** was reduced using NiCl₂·6H₂O and NaBH₄ then protected as the corresponding *t*-butyl

carbamate. Removal of the protecting group using trifluoroacetic acid in DCM provided amine **32**. The benzyl ether of **8v** was removed by hydrogenolysis in presence of Pd/C under a hydrogen atmosphere to yield **33**.

Finally, the synthesis of a benzoxaborole analogue is depicted in Scheme 5. A Mitsunobu reaction between 2-bromo-3-hydroxybenzaldehyde and (+)-methyl D-lactate was carried out in the presence of PPh₃ and DEAD in THF to give **34**. This aldehyde was treated with NaBH₄ in ethanol to generate the primary alcohol, which was protected as the corresponding methoxymethyl ether **35** using methoxymethyl chloride (MOMCl) and DIPEA in DCM. Boronylation of the aryl bromide was carried out using bis(pinacolato)diboron in the presence of KOAc and a catalytic amount of Pd(Ph₃P)₂Cl₂ in 1,4-dioxane to give **36**.⁴⁷ Ester hydrolysis followed by amine coupling with **5** (Ar = 4-CNPh) in the presence of EDC·HCl in DMF and then treatment with 6N HCl in THF gave benzoxaborole **37**.

Evaluation of *Mtb*IMPDPH2 inhibition.

We previously described the *Mtb*IMPDPH2 CBS inhibition and antibacterial activity of benzoxazole (**Q**) based inhibitors.³⁹ The most promising compounds, **2** and **3** (Figure 1A), had $K_{i,app}$ values of 76 nM and 14 nM, and MIC values of 16 μ M and 12 μ M, respectively. *Mtb*IMPDPH2 CBS was expressed and purified as previously described and the enzymatic activity was assayed by monitoring the production of NADH at sub-saturating NAD⁺ ($3 \times K_m$) and saturating IMP concentrations and 20–50 nM enzyme.⁹ The $K_{i,app}$ values reported herein were determined from the average of two independent experiments, unless otherwise noted. We also evaluated inhibition of the host enzymes *h*IMPDPH2 and *h*GMMPR2.

Initially, modifications of the pyridyl of **2** were evaluated (Table 1). Pyridine *N*-oxide **31** demonstrated comparable activity to the parent compound **2**. Addition of a methoxy to the pyridyl **8b** and **8c** resulted in 5-fold more inhibition than **2**. However, changing pyridyl to 2-pyridone (**30**) reduced inhibitory activity by 3-fold. Replacing pyridyl with phenyl having both electron donating groups (EDG) and electron withdrawing groups (EWG) was evaluated. Compounds **8d** (4-OMe), **8e** (4-OCF₃) and **8f** (4-CN) resulted in 7-fold increase in inhibitory activity compared to **2**. Fluorine (**8g**) and ester (**8h**) substituents were also tolerated. Replacing the pyridyl with a 4-hydroxy phenyl (**8i**) resulted in a 2-fold increase in inhibitory activity, whereas the 3-hydroxy (**8j**) and 2-hydroxy (**8k**) derivatives showed slightly decreased potency. Given the improved activity of **8d**, the effect of other ethers was examined. For example, **18a** and propargyl ester **20** shows a ~12-fold increase in activity compared to **2**, while the corresponding carboxylic acid (**19a**) and tetrazole (**27**) were moderately less potent. Translocating the alkoxy from the *para* to *meta* position resulted in a 4-fold loss in activity (**18b** and **19b**). Compounds containing hydrophilic substituents at the 4-position, such as hydroxamic acid **21**, carboxylic acid **22** and aminomethyl **29**, were found to be much less active. Replacing the carboxylate with hydrazide **23**, 1,3,4-oxadiazolone **24**, hydroxamidine **25**, 1,2,3-oxadiazolone **26** and primary amide **28** showed 2 to 7-fold increase in activity.

Previous work on the benzoxazole series had established that substitution at the 2- and 3-positions of aryl ether were important for inhibition of both *Cryptosporidium parvum*

IMPDH and *Mtb*IMPDH2 CBS.^{39,9} Several 2,3-dichlorophenyl compounds (**2**, **8c**, **8d**, **8f**, **8g** and **8i**) were compared to the corresponding 2,3-difluorophenyl analogues (**8l**, **8o**, **8m**, **8p**, **8q** and **8n**). Three of these compounds (**8l**, **8p** and **8q**) displayed similar activity whereas the others were 2 to 4-fold less active. Adding another substitution on the 4-position (**8r**) resulted in slightly reduced activity. Replacement of the 2-chlorophenyl with a 2-cyanophenyl (**8s** and **8t**) was well tolerated. In addition, compounds with 2-cyano (**8u**), 2-aminomethyl (**32**), and 2-hydroxy (**33**), and 2-benzyloxy (**8v**) substituents on the phenyl ether demonstrated *Mtb*IMPDH2 CBS $K_{i,app}$ values < 45 nM. However, the benzoxaborole (**37**) was not as well tolerated.

Several other areas of the **Q**-series were examined (Table 3). For example, the amide was replaced with a thioamide (**9**), which demonstrated a modest loss of activity. This decrease in potency is likely due a loss of a hydrogen bond to water, while retaining the ionic-dipole interaction between the thioamide NH and the carboxylate of Glu458. Furthermore, replacement of the amide with an amine (**11**) was not tolerated. In addition, activity was significantly decreased when the benzoxazole was replaced with an imidazo[1,2-a]pyridine (**13**). Adding a methylene between the phenyl and benzoxazole (**15**) also reduced activity by a factor of 6 compared to **8d**. However, replacing the aryl ether with aniline (**17a** and **17b**) resulted in increased inhibitory activity.

Selectivity of inhibition.

The cofactor binding sites are widely diverged in bacterial and eukaryotic IMPDHs, and the *Mtb*IMPDH2 inhibitors exploit this divergence^{9, 17}. Only four compounds, **8f**, **8p**, **17a** and **24**, modestly inhibited human IMPDH2, and in these cases selectivity ranged from a factor of 200 to 1000. No inhibition of human IMPDH2 was observed for the other compounds (maximum concentration tested was 5 μ M). GMP reductase (GMPR) is closely related to IMPDH, and catalyzes a similar reaction, the reduction of GMP by NADPH to produce IMP, NADP⁺ and ammonia⁴⁸. The adenosine site of human GMPR2 contains the Ala-Tyr motif that characterizes the inhibitor binding site of *Mtb*IMPDH2. However, none of the compounds inhibited human GMPR2 (maximum concentration tested was 5 μ M). These experiments demonstrate that compounds selectively inhibit bacterial IMPDHs and do not affect related host enzymes.

Evaluation of antibacterial activity.

Antibacterial activity was determined for *Mtb*IMPDH2 CBS inhibitors with $K_{i,app}$ 40 nM and selected additional compounds by monitoring the growth of *Mtb* H37Rv (ATCC 27294) after one week (Table 4). Since *in vitro* antibiotic efficacy can vary unpredictably with growth conditions,⁴⁹ antibacterial activity was assessed in both GAST/Fe and 7H9/ADC/Tween media, both of which lack purines (e.g. –Gua). Two compounds, **18a** and **20**, displayed MICs less than 1 μ M in both media. An additional 8 compounds, **8f**, **8l**, **8m**, **8p**, **8u**, **17a**, **17b** and **18b**, displayed MIC 5 μ M in both media. Six of these compounds retained antibacterial activity over two weeks: **8l**, **8u**, **17a**, **17b**, **18a** and **20**. Two compounds (**21** and **22**) were active in GAST/Fe medium (MIC 5 μ M) but considerably less effective in 7H9/ADC/Tween medium. These compounds also retained activity over two weeks.

Figure 3 shows the dependence of antibacterial activity on inhibition of *Mtb*IMPDPH2 CBS for the **Q** compounds described above as well as those reported previously⁹. Uptake and metabolism also play important roles in antibacterial efficacy, so it is not surprising that some potent *Mtb*IMPDPH2 CBS inhibitors fail to display antibacterial activity. Nonetheless, more potent enzyme inhibition is generally associated with greater antibacterial activity, as expected if antibacterial activity derived from inhibition of *Mtb*IMPDPH2.

Many bacteria have the ability to salvage guanine or guanosine, and thus overcome inhibition of IMPDH. *Mtb* can salvage guanine, but not guanosine, and previously reported IMPDH inhibitors were much less effective in the presence of high guanine concentrations^{9–11}. For example, the MIC values of indazole sulfonamide inhibitors of *Mtb*IMPDPH2 increased more than 25-fold in 100–125 μ M guanine^{10, 11}. Smaller increases were observed for previously reported **Q** compounds⁹. However, the MIC of only one of the new **Q** compounds, **8n**, increased substantially in the presence of guanine in both media. Intriguingly, this compound was one of the weaker inhibitors of *Mtb*IMPDPH2 ($K_{i,app} = 121$ nM). The MIC of one additional compound, **8c** ($K_{i,app} = 20$ nM), increased in the presence of guanine in 7H9/ADC/Tween medium but not in GAST/Fe. The failure of guanine to decrease the antibacterial activity of most **Q** compounds would usually suggest that antibacterial activity derives from the engagement of another target. Alternatively, guanine salvage may not be sufficient to support growth in the presence of potent *Mtb*IMPDPH2 inhibition. It is also possible that the **Q** inhibitors stabilize/disrupt a protein complex, thereby perturbing a moonlighting activity of *Mtb*IMPDPH2 in addition to enzyme activity.

We performed two experiments to further address the question of whether antibacterial activity derived from on-target inhibition of *Mtb*IMPDPH2. First, we evaluated the effect of *Mtb*IMPDPH2 depletion on the antibacterial activity of four *Mtb*IMPDPH2 inhibitors, including one compound with guanine-dependent antibacterial activity (**1**)⁹, and three compounds with guanine-independent antibacterial activity (**17b**, **18a** and **22**; note that **22** is only active in GAST/Fe). The downregulation of *Mtb*IMPDPH2 was achieved using strain *guaB2* cKD, in which *guaB2* expression is suppressed by anhydrotetracycline (ATc).¹¹ The antibacterial activities of **1**, **17b**, **18a**, and **22** against the wild-type strain were not affected by the addition of ATc (Table 5). In contrast, treatment with ATc hypersensitized the *guaB2* cKD strain to all four compounds (Figure 4), suggesting that antibacterial activity derives primarily from the inhibition of *Mtb*IMPDPH2.

The antibacterial activity of **1**, **17b**, **18a**, and **22** was also assessed against *Mtb* strain SRMV2.6. This strain expresses the mutant *Mtb*IMPDPH2/Y487C, which is resistant to an isoquinoline sulfonamide inhibitor¹¹. As noted above, Tyr487 interacts with the benzoxazole group, so the substitution of Cys is expected to disrupt the binding of all the **Q** inhibitors. SRMV2.6 was resistant to **1** and **17b** (Table 5), further confirming that the antibacterial activity of these compounds resulted from on-target inhibition of *Mtb*IMPDPH2. Interestingly, however, SRMV2.6 remained sensitive to **18a** and **22**.

We measured the inhibition of recombinant *Mtb*IMPDPH2/Y487C to determine if the Y487C mutation decreased the affinity of all the **Q** compounds as expected (Table 5). The values of $K_{i,app}$ for **1** and **17b** were increased by more than 300-fold and 60-fold, respectively, which

can account for the resistance of strain SRMV2.6. These observations further confirm that the antibacterial activity of **1** and **17b** derive from inhibition of *Mtb*IMPDH2. The values of $K_{i,app}$ for **18a** and **22** were similarly increased in *Mtb*IMPDH2/Y487C, by at least 2000-fold and approximately 40-fold, respectively. These observations suggest that strain SRMV2.6 should also be resistant to **1** and **18a**, yet it remained sensitive to these compounds. Perhaps **1** and **18a** are concentrated or metabolized in the bacteria, or perhaps these compounds interfere with a moonlighting function. Alternatively, these compounds may engage an additional target(s). Irrespective of the ambiguous mechanism of action of **1** and **18a**, **17b** demonstrates that on-target inhibition of *Mtb*IMPDH2 can be impervious to guanine rescue, suggesting that it is a vulnerable target.

Evaluation of Human Cytotoxicity Activity.

Compounds displaying potent antibacterial activity (**8l**, **8p**, **8u**, **17b**, **18a** and **20**) were evaluated for cytotoxicity against HepG2 cells using a LDH release assay. Only compounds **8p**, **8u** and **17b** displayed measurable cytotoxicity (9–13% lactate dehydrogenase release) at 25 μ M ($LD_{50} > 25 \mu$ M, Figure 5). Since **18a** and **20** are esters of **19a**, we also examined the cytotoxicity of this compound, and again no cytotoxicity was observed. The cytotoxicity of **17b** (25 μ M) was also less than 10% in HeLa, HEK293T and MCF7 cells. These experiments demonstrate that all of the compounds display a greater than 10-fold selectivity for antibacterial activity versus cytotoxicity (the recommended criteria for *Mtb*⁵⁰), with the selectivity of some exceeding 100-fold.

Preliminary pharmacokinetic evaluation of 17b.

The above observations prompted us to consider evaluating the pharmacokinetics of **17b** and **18a** as a prelude to possible testing in a mouse model of tuberculosis. We first evaluated the stability of **17b** and **18a** in mouse liver microsomes. **18a** was rapidly metabolized ($t_{1/2} = 1.3$ min) in an NADPH-independent process. Compound **19a**, the ester of **18a** was also metabolized in an NADPH-independent process, although with a much longer half-life ($t_{1/2} = 23$ min). These observations suggest that both the ester and amide bonds of **18a** may be liabilities. Compound **17b** was metabolized in an NADPH-dependent process with $t_{1/2} = 26$ min. No decomposition of **17b** was observed when it was incubated in mouse plasma at 37 °C for 2 h. Based on these results **17b** was selected for further analysis. This compound displayed promising pharmacokinetics in mice, with a single 20 mg/kg oral dose [formulated using Tween 80 (1%) and 0.5% (w/v) methylcellulose in water (99%)] producing a maximum plasma concentration level comparable to MIC ($C_{max} = 3 \mu$ M) in 0.5 h (T_{max}) with a plasma elimination half-life of 5 h. However, **17b** also displays high serum protein binding (>99%), which suggests that the free drug concentration is insufficient to achieve in vivo efficacy. Further optimization of **17b** to increase antibacterial activity and decrease plasma protein binding is ongoing.

CONCLUSIONS

The SAR of the benzoxazole-based IMPDH inhibitors (**Q**-series) has been expanded by replacing the 4-pyridyl with phenyl or benzyl groups containing a variety of hydrogen bonding and ionic-dipole interacting substituents. Modifications to the central amide and

benoxazole also reinforced the importance of interactions between the inhibitors and Glu458, and the spatial orientation provided by the central heterocycle, respectively. Two *Mtb*IMPDH2 inhibitors displayed antibacterial activity with MIC values $\approx 1 \mu\text{M}$, and another eight compounds displayed MICs $\approx 5 \mu\text{M}$. The antibacterial activity of the best candidate, **17b**, derives from inhibition of *Mtb*IMPDH2, yet is not affected by the presence of guanine. This observation alleviates the concern that guanine salvage can rescue bacteria from *Mtb*IMPDH2 inhibition. We note that previously reported *Mtb*IMPDH2 inhibitors were not as potent as the current compounds, and suggest that the ability of guanine to protect bacteria derived from incomplete inhibition of *Mtb*IMDPH2. The values of $K_{i,\text{app}}$ for the best inhibitors are 25-fold more potent than the indazole sulfonamide inhibitor that called into question the vulnerability of *Mtb*IMPDH2,¹⁰ suggesting that guanine salvage cannot overcome potent inhibition. **17b** was also non-toxic at $25 \mu\text{M}$ in four human cell lines. Overall, this study provides further evidence for the vulnerability of *Mtb*IMPDH2.

Experimental Section

Synthetic Chemistry.—Unless otherwise noted, all reagents and solvents were purchased from commercial sources and used without further purification. All reactions were performed under a nitrogen atmosphere in dried glassware unless otherwise noted. All NMR spectra were obtained using a 400 MHz spectrometer. For ^1H NMR, all chemical shifts are reported in δ units ppm and are referenced to tetramethylsilane (TMS). All chemical shift values are also reported with multiplicity, coupling constants, and proton count. Coupling constants (J) are reported in hertz. Column chromatography was carried out on SILICYCLE SiliaFlash silica gel F60 (40–63 μm , mesh 230–400). High-resolution mass spectra were obtained using a Q-tof UE521 mass spectrometer (University of Illinois, SCS, and Mass Spectrometry Laboratory). HPLC conditions: All final compounds have a chemical purity of >98% as determined by analysis using a Varian Prostar (380-LC) HPLC instrument equipped with a quaternary pump and a Varian Microsorb MV-100–5 C-8 column (250 mm \times 4.6 mm). UV absorption was monitored at 332 nm. All samples were dissolved in THF (1–2 mg/mL) and the injection volume was 20 μL . HPLC gradient was 30% acetonitrile and 70% water (both solvents contain 0.05% formic acid) with a total run time of 20 min and a flow rate of 1.0 mL/min.

General Procedure for the Synthesis of 5-nitro-2-phenylbenzo[d]oxazoles

(4): To a stirred solution of 2-amino-4-nitrophenol (1 mmol) and aromatic aldehydes (1 mmol) in anhydrous xylene DarcoKB (300 mg) was added. The solution was stirred under O_2 atmosphere at 140°C for 6–8 h. After completion of the reaction as observed from TLC, reaction mixture was filtered with the aid of Celite, which was washed with hot ethyl acetate (3 \times 20 mL). The filtrate was concentrated, and the products were either used directly or recrystallized using ethyl acetate and hexane.

General Procedure for the Synthesis of 5: 5-Nitro-2-arylbenzo[d]oxazole **4** (1 mmol) was dissolved in 10 mL EtOAc:MeOH (1:1) and 10% Pd/C (catalytic) was added and stirred well under a H_2 atmosphere for 3 h. After the successful completion, the reaction mixture was filtered through celite and the filtrate was concentrated under reduced pressure. The crude amines were used directly or recrystallized using ethyl acetate and hexane.

General Procedure for the Synthesis of Phenyl Ethers 6: Substituted phenol (1 mmol) was added to the solution of methyl (+)-methyl D-lactate (1.38 mmol) in anhydrous THF (6 mL) under a nitrogen atmosphere. The solution was cooled to 0 °C, followed by PPh₃ (1.20 mmol) was added portion wise to the stirred solution. DEAD (1.50 mmol) was added dropwise to the above solution and stirred well at room temperature for 4 h. After completion, solvent was removed under reduced pressure and the crude residue was purified by column chromatography on silica gel using ethyl acetate/n-hexane (10:90) to yield corresponding phenyl ether as a colorless liquid (85–90% Yield).

General Procedure for Ester Hydrolysis for Preparation of 7: LiOH (1.5 mmol) was added portion wise to the stirred solution of ester **6** (1 mmol) in 5 mL THF:MeOH (2:3) at 0 °C. The reaction was brought to room temperature and stirred well for 4 h. The solvents were removed under reduced pressure, 1N HCl was added to a pH of 4 and then the mixture was extracted with ethyl acetate. The organic layer was washed with brine, dried using anhydrous MgSO₄, filtered, and concentrated under reduced pressure. The crude acids were used in the next step without purification.

(S)-2-(2,3-Dichlorophenoxy)-N-(2-(pyridin-4-yl)benzo[d]oxazol-5-yl)propanamide (8a): Prepared and characterized previously.³⁹

General Procedure for Synthesis of 8b-8v: EDC·HCl (1.5 mmol) was added to the stirred solution of acid **7** (1 mmol) and amine **5** (1 mmol) in dry DMF at 0 °C under nitrogen atmosphere. The reaction mixture was stirred overnight at room temperature. After completion of the reaction, excess water was added and extracted with ethyl acetate. The organic layer was washed with brine and dried using anhydrous MgSO₄. The solvent was removed under reduced pressure and the crude residue was purified through column chromatography using ethyl acetate/n-hexane.

(S)-2-(2,3-Dichlorophenoxy)-N-(2-(2-methoxy pyridin-4-yl)benzo[d]oxazol-5-yl)propanamide (8b): White solid (306 mg, 66%), ¹H NMR (DMSO-*d*₆) 10.34 (s, 1H, NH), 8.93 (d, *J* = 2.00 Hz, 1H, CH), 8.39–8.36 (m, 1H, CH), 8.06 (d, *J* = 2.00 Hz, 1H, CH), 7.69 (d, *J* = 8.80 Hz, 1H, CH), 7.52 (dd, *J* = 8.90 Hz, *J* = 2.00 Hz, 1H, CH), 7.30–7.26 (m, 1H, CH), 7.22 (t, *J* = 1.20 Hz, 1H, CH), 7.02–7.00 (m, 2H, 2×CH), 4.98 (q, *J* = 6.80 Hz, 1H, CH), 3.92 (s, 3H, -OCH₃), 1.59 (d, *J* = 6.80 Hz, 3H, CH₃). Purity 98% (t_R = 15.13). m.p. 165–166 C.

(S)-2-(2,3-dichlorophenoxy)-N-(2-(6-methoxy pyridin-3-yl)benzo[d]oxazol-5-yl)propanamide (8c): White solid (315 mg, 69%), ¹H NMR (DMSO-*d*₆) 10.34 (s, 1H, NH), 8.92 (m, 1H, CH), 8.39–8.37 (m, 1H, CH), 8.06–8.05 (m, 1H, CH), 7.69–7.67 (m, 1H, CH), 7.53–7.51 (m, 1H, CH), 7.27–7.20 (m, 2H, 2×CH), 7.01–6.98 (m, 2H, 2×CH), 5.01 (q, *J* = 6.80 Hz, 1H, CH), 3.91 (s, 3H, -OCH₃), 1.58 (d, *J* = 6.80 Hz, 3H, CH₃). Purity 97% (t_R = 14.85). m.p. 156–157 C.

(S)-2-(2,3-Dichlorophenoxy)-N-(2-(4-methoxyphenyl)benzo[d]oxazol-5-yl)propanamide (8d): White solid (351 mg, 77%), ¹H NMR (DMSO-*d*₆) 10.32 (s, 1H, NH), 8.08 (d, *J* = 8.80 Hz, 2H, 2×CH), 8.03 (d, *J* = 2.00 Hz, 1H, CH), 7.65 (d, *J* = 8.80 Hz,

1H, CH), 7.50–7.48 (m, 1H, CH), 7.27 (t, $J = 8.20$ Hz, 1H, CH), 7.21–7.19 (m, 1H, CH), 7.10 (d, $J = 8.80$ Hz, 2H, 2×CH), 7.01–6.99 (m, 1H, CH), 4.98 (q, $J = 6.80$ Hz, 1H, CH), 3.82 (s, 3H, -OCH₃), 1.59 (d, $J = 6.80$ Hz, 3H, CH₃). Purity 99% ($t_R = 15.30$). m.p. 230 C.

(S)-2-(2,3-Dichlorophenoxy)-N-(2-(4-(trifluoromethoxy)phenyl)benzo[d]oxazol-5-yl)propanamide (8e): White solid (357 mg, 70%), ¹H NMR (DMSO-*d*₆) 10.41 (s, 1H, NH), 8.31 (d, $J = 8.80$ Hz, 2H, 2×CH), 8.16 (m, 1H, CH), 7.77 (d, $J = 9.00$ Hz, 1H, CH), 7.61 (d, $J = 8.00$ Hz, 2H, 2×CH), 7.59 (m, 1H), 7.32 (t, $J = 8.20$ Hz, 1H, CH), 7.26–7.24 (m, 1H, CH), 7.05 (d, $J = 6.40$ Hz, 1H, CH), 5.03 (q, $J = 6.20$ Hz, 1H, CH), 1.64 (d, $J = 6.40$ Hz, 3H, CH₃). Purity 99% ($t_R = 17.15$). m.p. 140–141 C.

(S)-N-(2-(4-Cyanophenyl)benzo[d]oxazol-5-yl)-2-(2,3-dichlorophenoxy)propanamide (8f): Yellow solid (311 mg, 69%), ¹H NMR (DMSO-*d*₆) 10.38 (s, 1H, NH), 8.28 (dd, $J = 8.20$ Hz, $J = 1.20$, 2H, 2×CH), 8.14 (m, 1H, CH), 8.02 (dd, $J = 8.20$ Hz, $J = 1.20$ Hz, 2H, 2×CH), 7.75–7.73 (m, 1H, CH), 7.58–7.56 (m, 1H, CH), 7.26 (t, $J = 1.60$ Hz, 1H, CH), 7.20 (m, 1H, CH), 7.00 (d, $J = 8.40$ Hz, 1H, CH), 5.01 (q, 1H, $J = 6.80$ Hz, CH), 1.58 (d, 3H, $J = 6.80$ Hz, CH₃). Purity 99% ($t_R = 14.85$). m.p. 183–184 C.

(S)-2-(2,3-Dichlorophenoxy)-N-(2-(4-fluorophenyl)benzo[d]oxazol-5-yl)propanamide (8g): White solid (351 mg, 79%), ¹H NMR (DMSO-*d*₆) 10.42 (s, 1H, NH), 8.26–8.23 (m, 2H, 2×CH), 8.13 (m, 1H, CH), 7.76–7.74 (m, 1H, CH), 7.59–7.44 (m, 3H, 3×CH), 7.32–7.26 (m, 2H, 2×CH), 7.06–7.04 (m, 1H, CH), 5.04 (q, $J = 6.00$ Hz, 1H, CH), 1.64 (d, $J = 6.00$ Hz, 3H, CH₃). Purity 98% ($t_R = 15.73$). m.p. 213–214 C.

Methyl (S)-4-(5-(2-(2,3-dichlorophenoxy)propanamido)benzo[d]oxazol-2-yl)benzoate (8h): White solid (329 mg, 68%), ¹H NMR (DMSO-*d*₆) 10.37 (s, 1H, NH), 8.29–8.26 (m, 1H, CH), 8.11 (d, $J = 8.80$ Hz, 2H, 2×CH), 7.86 (m, 1H, CH), 7.73 (dd, $J = 8.80$ Hz, $J = 3.20$ Hz, 1H, CH), 7.56 (d, $J = 8.20$ Hz, 1H, CH), 7.40 (m, 1H, CH), 7.27–7.20 (m, 2H, 2×CH), 7.00 (dd, $J = 8.80$ Hz, $J = 2.00$ Hz, 1H, CH), 5.02 (q, 1H, $J = 6.80$ Hz, 1H, CH), 3.85 (s, 3H, -COOCH₃), 1.59 (d, 3H, $J = 6.00$ Hz, CH₃). Purity 99% ($t_R = 15.60$). m.p. 197–198 C.

(S)-2-(2,3-Dichlorophenoxy)-N-(2-(4-hydroxyphenyl)benzo[d]oxazol-5-yl)propanamide (8i): White solid (313 mg, 71%), ¹H NMR (DMSO-*d*₆) 10.30 (s, 1H, NH), 8.00–7.99 (m, 1H, CH), 7.97 (d, $J = 8.40$ Hz, 2H, 2×CH), 7.62 (d, $J = 8.80$ Hz, 1H, CH), 7.48–7.46 (m, 1H, CH), 7.27 (t, $J = 8.00$ Hz, 1H, CH), 7.00 (d, $J = 8.40$ Hz, 1H, CH), 6.91 (d, $J = 8.80$ Hz, 2H, 2×CH), 4.47 (q, $J = 6.40$ Hz, 1H, CH), 1.58 (d, $J = 6.80$ Hz, 3H, CH₃). Purity 99% ($t_R = 13.11$). m.p. 213.5–214.5 C.

(S)-2-(2,3-Dichlorophenoxy)-N-(2-(3-hydroxyphenyl)benzo[d]oxazol-5-yl)propanamide (8j): White solid (300 mg, 68%), ¹H NMR (DMSO-*d*₆) 10.38 (s, 1H, NH), 9.75 (s, 1H, OH), 8.12 (s, 1H, CH), 7.74 (d, $J = 9.20$ Hz, 1H, CH), 7.61–7.55 (m, 3H, 3×CH), 7.40 (t, $J = 8.00$ Hz, 1H, CH), 7.32 (t, $J = 8.20$ Hz, 1H, CH), 7.26 (m, 1H), 7.06–

7.01 (m, 2H, 2×CH), 5.03 (q, $J = 6.80$ Hz, 1H, CH), 1.64 (d, $J = 6.40$ Hz, 3H, CH₃). Purity 98% ($t_R = 13.36$). m.p. 259 C.

(S)-2-(2,3-Dichlorophenoxy)-N-(2-(2-hydroxyphenyl)benzo[d]oxazol-5-yl)propanamide (8k): White solid (287 mg, 65%), ¹H NMR (DMSO-*d*₆) 11.10 (s, 1H, OH), 10.41 (s, 1H, NH), 8.13 (d, $J = 2.00$ Hz, 1H, CH), 7.97 (dd, $J = 7.60$ Hz, $J = 1.20$ Hz, 1H, CH), 7.76 (d, $J = 8.40$ Hz, 1H, CH), 7.55 (dd, $J = 8.40$ Hz, $J = 2.00$ Hz, 1H, CH), 7.54–7.48 (m, 1H, CH), 7.26 (t, $J = 8.00$ Hz, 1H, CH), 7.19 (m, 1H, CH), 7.09–7.00 (m, 3H, 3×CH), 5.00 (q, $J = 6.80$ Hz, 1H, CH), 1.59 (d, $J = 6.60$ Hz, 3H, CH₃). Purity 99% ($t_R = 16.99$). m.p. 209–210 C.

(S)-2-(2,3-Difluorophenoxy)-N-(2-(pyridin-4-yl)benzo[d]oxazol-5-yl)propanamide (8l): White solid (268 mg, 68%), ¹H NMR (DMSO-*d*₆) 10.40 (s, 1H, NH), 8.79 (dd, $J = 4.20$ Hz, $J = 1.20$ Hz, 2H, CH), 8.16 (m, 1H, CH), 8.04 (t, $J = 2.00$ Hz, 2H, 2×CH), 7.77 (d, $J = 8.80$ Hz, 1H, CH), 7.62 (m, 1H, CH), 7.62–7.60 (m, 1H, CH), 4.96 (q, $J = 6.80$ Hz, 1H, CH), 1.58 (d, $J = 6.80$ Hz, 3H, CH₃). Purity 99% ($t_R = 14.45$). m.p. 189–190 C.

(S)-2-(2,3-Difluorophenoxy)-N-(2-(4-methoxyphenyl)benzo[d]oxazol-5-yl)propanamide (8m): White solid (322 mg, 76%), ¹H NMR (DMSO-*d*₆) 10.32 (s, 1H, NH), 8.08 (d, $J = 9.20$ Hz, 2H, 2×CH), 8.02 (d, $J = 1.60$ Hz, 1H, CH), 7.64 (d, $J = 8.40$ Hz, 1H, CH), 7.50 (d, $J = 6.80$ Hz, 1H, CH), 7.10 (d, $J = 8.80$ Hz, 3H, 3×CH), 6.99 (m, 1H, CH), 6.89 (t, $J = 2.00$ Hz, 1H, CH), 4.95 (q, $J = 6.80$ Hz, 1H, CH), 1.57 (d, $J = 6.40$ Hz, 3H, CH₃). Purity 97% ($t_R = 13.95$). m.p. 179–180 C.

(S)-2-(2,3-Difluorophenoxy)-N-(2-(4-hydroxyphenyl)benzo[d]oxazol-5-yl)propanamide (8n): White solid (291 mg, 71%), ¹H NMR (DMSO-*d*₆) 10.36 (s, 1H, OH), 10.33 (s, 1H, NH), 8.04 (d, $J = 2.00$ Hz, 2H, 2×CH), 8.01 (m, 1H, CH), 7.67 (d, $J = 8.80$ Hz, 1H, CH), 7.52 (d, $J = 8.20$ Hz, 1H, CH), 7.15–6.97 (m, 3H, 3×CH), 6.96 (d, $J = 8.40$ Hz, 2H, 2×CH), 4.99 (q, 1H, $J = 6.80$ Hz, CH), 1.62 (d, 3H, $J = 6.40$ Hz, CH₃). Purity 98% ($t_R = 11.36$). m.p. 182–183 C.

(S)-2-(2,3-Difluorophenoxy)-N-(2-(6-methoxypyridin-3-yl)benzo[d]oxazol-5-yl)propanamide (8o): White solid (311 mg, 69%), ¹H NMR (DMSO-*d*₆) 10.49 (s, 1H, NH), 8.97 (s, 1H, CH), 8.40 (dd, $J = 8.40$ Hz, $J = 2.00$ Hz, 1H, CH), 8.11 (m, 1H, CH), 7.73 (d, $J = 8.00$ Hz, 1H, CH), 7.59–7.56 (m, 1H, CH), 7.19–6.98 (m, 3H, 3×CH), 6.94 (t, $J = 2.40$ Hz, 1H, CH), 5.00 (q, $J = 6.40$ Hz, 1H, CH), 3.17 (s, 3H, -OCH₃), 1.63 (d, $J = 6.40$ Hz, 3H, CH₃). Purity 99% ($t_R = 13.25$). m.p. 177–178 C.

(S)-N-(2-(4-Cyanophenyl)benzo[d]oxazol-5-yl)-2-(2,3-difluorophenoxy)propanamide (8p): White solid (289 mg, 69%), ¹H NMR (DMSO-*d*₆) 10.44 (s, 1H, NH), 8.34 (d, $J = 8.40$ Hz, 2H, 2×CH), 8.19 (d, $J = 1.60$ Hz, 1H, CH), 8.07 (d, $J = 8.8$ Hz, 2H, 2×CH), 7.79 (d, $J = 8.80$ Hz, 1H, CH), 7.65–7.62 (m, 1H, CH), 7.17–7.12 (m, 1H, CH), 7.06–7.02 (m, 1H, CH), 6.95 (t, $J = 2.00$ Hz, 1H, CH), 5.01 (q, $J = 6.40$ Hz, 1H, CH), 1.63 (d, $J = 6.8$ Hz, 3H, CH₃). Purity 98% ($t_R = 13.24$). m.p. 176–177 C.

(S)-2-(2,3-Difluorophenoxy)-N-(2-(4-fluorophenyl)benzo[d]oxazol-5-yl)propanamide (8q): White solid (317 mg, 77%), ¹H NMR (DMSO-*d*₆) 10.40 (s, 1H, NH), 8.24 (dd, *J* = 8.60 Hz, *J* = 5.40 Hz, 2H, 2×CH), 8.13 (d, *J* = 1.60 Hz, 1H, CH), 7.74 (d, *J* = 9.20 Hz, 1H, CH), 7.58 (dd, *J* = 8.80 Hz, *J* = 2.00 Hz, 1H, CH), 7.46 (td, *J* = 8.80, *J* = 1.00 Hz, 2H, 2×CH), 7.17–7.12 (m, 1H, CH), 7.06–7.02 (m, 1H, CH), 6.96–6.92 (m, 1H, CH), 5.00 (q, *J* = 6.40 Hz, 1H, CH), 1.63 (d, *J* = 6.80 Hz, 3H, CH₃). Purity 97% (t_R = 14.29). m.p. 194–195 C.

(S)-N-(2-(4-Cyanophenyl)benzo[d]oxazol-5-yl)-2-(2,3,4-trifluorophenoxy)propanamide (8r): White solid (270 mg, 62%), ¹H NMR (DMSO-*d*₆) 10.42 (s, 1H, NH), 8.34 (d, *J* = 6.80 Hz, 2H, 2×CH), 8.19 (s, 1H, CH), 8.08 (d, *J* = 7.20 Hz, 2H, 2×CH), 7.80 (d, *J* = 8.00 Hz, 1H, CH), 7.63 (d, *J* = 8.40 Hz, 1H, CH), 7.27 (d, *J* = 10.00 Hz, 1H, CH), 6.98 (m, 1H, CH), 4.98 (q, *J* = 6.40 Hz, 1H, CH), 1.61 (d, *J* = 6.80 Hz, 3H, CH₃). Purity 99% (t_R = 13.60). m.p. 184–185 C.

(S)-2-(2-Cyanophenoxy)-N-(2-(pyridin-4-yl)benzo[d]oxazol-5-yl)propanamide (8s): White solid (261 mg, 68%), ¹H NMR (DMSO-*d*₆) 10.49 (s, 1H, NH), 8.84 (dd, *J* = 4.00 Hz, *J* = 1.60 Hz, 2H, 2×CH), 8.21 (d, *J* = 2.00 Hz, 1H, CH), 8.09 (dd, *J* = 4.40 Hz, *J* = 1.60 Hz, 2H, 2×CH), 7.83–7.77 (m, 2H, 2×CH), 7.68–7.63 (m, 2H, 2×CH), 7.14–7.11 (m, 2H, 2×CH), 5.11 (q, *J* = 6.80 Hz, 1H, CH), 1.66 (d, *J* = 6.80 Hz, 3H, CH₃). Purity 98% (t_R = 12.67). m.p. 229–230 C.

(S)-2-(2-Cyano-3-fluorophenoxy)-N-(2-(pyridin-4-yl)benzo[d]oxazol-5-yl)propanamide (8t): White solid (285 mg, 71%), ¹H NMR (DMSO-*d*₆) 10.51 (s, 1H, NH), 8.84 (dd, *J* = 6.00 Hz, *J* = 1.00 Hz, 2H, 2×CH), 8.20 (s, 1H, CH), 8.09 (dd, *J* = 6.00 Hz, *J* = 1.00 Hz, 2H, 2×CH), 7.84–7.81 (m, 1H, CH), 7.73–7.63 (m, 2H, 2×CH), 7.10 (t, *J* = 8.80 Hz, 1H, CH), 6.99–6.97 (d, *J* = 8.80 Hz, 1H, CH), 5.16 (q, *J* = 6.40 Hz, 1H, CH), 1.67 (d, *J* = 6.80 Hz, 3H, CH₃). Purity 98% (t_R = 13.44). m.p. 189–dec C.

(S)-2-(2-Cyanophenoxy)-N-(2-(4-methoxyphenyl)benzo[d]oxazol-5-yl)propanamide (8u): White solid (318 mg, 77%), ¹H NMR (DMSO-*d*₆) 10.41 (s, 1H, NH), 8.13 (d, *J* = 8.80 Hz, 2H, 2×CH), 8.07 (m, 1H, CH), 7.78 (d, *J* = 8.80 Hz, 1H, CH), 7.72 (m, 2H, 3×CH), 7.54 (d, *J* = 8.00 Hz, 1H, CH), 7.21–7.04 (m, 4H, 4×CH), 5.09 (q, *J* = 6.00 Hz, 1H, CH), 3.82 (s, 3H, OCH₃), 1.65 (d, *J* = 6.40 Hz, 3H, CH₃). Purity 99% (t_R = 12.99). m.p. 162–163 C.

(S)-2-(2-(Benzyloxy)phenoxy)-N-(2-(4-cyanophenyl)benzo[d]oxazol-5-yl)propanamide (8v): White solid (337 mg, 69%), ¹H NMR (DMSO-*d*₆) 10.23 (s, 1H, NH), 8.34 (d, *J* = 8.00 Hz, 2H, 2×CH), 8.21 (m, 1H, CH), 8.08 (d, *J* = 8.00 Hz, 2H, 2×CH), 7.76 (d, *J* = 8.80 Hz, 1H, CH), 7.61–7.58 (m, 1H, CH), 7.50 (d, *J* = 7.60 Hz, 2H, 2×CH), 7.38–7.29 (m, 3H, 3×CH), 7.08 (m, 2H, 2×CH), 6.93 (m, 2H, 2×CH), 5.17 (s, 2H, -OCH₂-), 4.82 (q, *J* = 6.40 Hz, 1H, CH), 1.57 (d, *J* = 6.80 Hz, 3H, CH₃). Purity 99% (t_R = 15.31). m.p. 144–145 C.

(S)-2-(2,3-Dichlorophenoxy)-N-(2-(4-methoxyphenyl)benzo[d]oxazol-5-yl)propanethioamide (9): A mixture of amide **8** (Ar = 4-OMePh, R = 2,3-diCl, 1 mmol)

and Lawesson's reagent (1 mmol) was dissolved in dry dioxane (5 mL) and refluxed well for 2h. After cooling to room temperature, dioxane was removed under reduced pressure and the crude product was purified through column chromatography. White solid (335 mg, 71%), ¹H NMR (DMSO-*d*₆) 11.72 (s, 1H, NH), 8.10–8.08 (m, 3H, 3×CH), 7.76–7.70 (m, 1H, CH), 7.51–7.50 (m, 1H, CH), 7.32–7.29 (m, 1H, CH), 7.22–7.20 (m, 1H, CH), 7.14–7.02 (m, 2H, 2×CH), 7.02–7.00 (m, 1H, CH), 5.20 (q, *J* = 6.80 Hz, 1H, CH), 1.70 (d, *J* = 6.80 Hz, 3H, CH₃). Purity 98% (*t*_R = 17.09). m.p. 132–139 C.

(S)-2-(2,3-Dichlorophenoxy)propanal (10): DIBAL-H (1.0 M, in cyclohexane, 2 mmol) was added dropwise to the stirred solution of ester **6a** (1 mmol) in dry CH₂Cl₂ (4 mL) under a nitrogen atmosphere at –78 °C. After completion of the addition, stirring was continued at the same temperature for 1 h. Aq. HCl (1 N, 3 mL) was added carefully. The bath was removed and the mixture was extracted with Et₂O (3 ×30 mL). The combined organic layers were washed with water (10 mL) and brine (10 mL) and dried over anhydrous MgSO₄. The solvent was removed under reduced pressure and the crude reaction mixture was purified through column chromatography. Colorless oil (193 mg, 89%), ¹H NMR (CDCl₃) 9.72 (s, 1H, CH), 7.10 (m, 2H, 2×CH), 6.74–6.71 (m, 1H, CH), 4.62–4.60 (m, 1H, CH), 1.51 (d, *J* = 7.20 Hz, 3H, CH₃).

(S)-N-(2-(2,3-Dichlorophenoxy)propyl)-2-(4-methoxyphenyl)benzo[d]oxazol-5-amine (11): Aldehyde **10** (1 mmol) was dissolved in DCE (25 mL) at 0 °C. Benzoxazole amine **5** (Ar = 4-OMePh, 1 mmol) and sodium triacetoxyborohydride (2 mmol) were added to the above solution and stirred well. The reaction mixture was stirred for 1.5 h and quenched with satd. NaHCO₃ solution (20 mL), and the product was extracted with CH₂Cl₂ (2 × 20 mL). The organic layer was washed with brine and dried using anhydrous MgSO₄. The solvent was removed under reduced pressure and crude mixture was purified through column chromatography. Colorless oil (351 mg, 81%), ¹H NMR (CDCl₃) 8.11 (dd, *J* = 9.20 Hz, *J* = 2.00 Hz, 2H, 2×CH), 7.29 (dd, *J* = 8.80 Hz, *J* = 2.40 Hz, 1H, CH), 7.05–7.02 (m, 2H, 2×CH), 6.96 (dd, *J* = 9.00 Hz, *J* = 2.60 Hz, 2H, 2×CH), 6.92–6.91 (m, 1H, CH), 6.81–6.78 (m, 1H, CH), 6.59 (dd, *J* = 8.60 Hz, *J* = 2.20 Hz, 1H, CH), 4.64 (m, 1H, CH), 4.21 (bs, 1H, NH), 3.84 (s, 3H, -OCH₃), 3.47–3.39 (m, 2H, -CH₂-), 1.39 (d, *J* = 6.20 Hz, 3H, CH₃). Purity 98% (*t*_R = 17.11).

2-(4-Methoxyphenyl)-6-nitroimidazo[1,2-a]pyridine (12): 5-Nitropyridin-2-amine (1 mmol) and NaHCO₃ (2 mmol) was added to a stirred solution of 2-bromo-4'-methoxyacetophenone (1 mmol) in ethanol at room temperature and the reaction mixture was refluxed for overnight. After completion, the solvent was removed under reduced pressure and the crude material was dissolved in water and extracted with ethyl acetate. The organic layer was washed with brine and dried using anhydrous MgSO₄, filtered and concentrated under reduced pressure. The product was recrystallized using ethyl acetate and hexane. Brown solid (237 mg, 88%), ¹H NMR (DMSO-*d*₆) 9.76 (m, 1H, CH), 8.47 (s, 1H, CH), 7.90–7.88 (m, 3H, 3×CH), 7.67–7.65 (m, 1H, CH), 7.61 (d, 2H, *J* = 8.80 Hz, 2×CH), 3.78 (s, 3H, -OCH₃).

(S)-2-(2,3-Dichlorophenoxy)-N-(2-(4-methoxyphenyl)imidazo[1,2-a]pyridin-6-yl)propanamide (13): To the stirred solution of 2-(4-methoxyphenyl)-6-nitroimidazo[1,2-a]pyridine **12** (1 mmol) in ethanol and ethyl acetate, SnCl₂ (2 mmol) was added and refluxed for 2h. Solvent was removed under reduced pressure and the reaction was quenched by adding a saturated solution of NaHCO₃ solution and extracted with ethyl acetate. The organic phase was washed with brine, dried over anhydrous MgSO₄, filtered and concentrated under reduced pressure. The crude amine was used in the next step without any purification. EDC·HCl (1.5 mmol) was added to the stirred solution of acid **7** (R = 2,3-diCl, 1 mmol) and amine (1 mmol) in dry DMF at 0 °C under a nitrogen atmosphere. The reaction mixture was stirred overnight at room temperature. After completion of the reaction, water was added and extracted with ethyl acetate. The organic layer was washed with brine and dried using anhydrous MgSO₄. The solvent was removed under reduced pressure. The crude residue was purified through column chromatography to give the desired product. Brown solid (273 mg, 60%), ¹H NMR (DMSO-*d*₆) 10.35 (s, 1H, NH), 9.13 (s, 1H, CH), 8.33 (s, 1H, CH), 7.84 (d, *J* = 8.40 Hz, 2H, 2×CH), 7.53 (d, *J* = 8.00 Hz, 1H, CH), 7.24–6.92 (m, 6H, 6×CH), 5.02 (q, *J* = 6.40 Hz, 1H, CH), 3.79 (s, 3H, -OCH₃), 1.62 (d, *J* = 6.40 Hz, 3H, CH₃). Purity 97% (t_R = 12.00). m.p. 146–147 C.

2-(4-Methoxybenzyl)-5-nitrobenzo[d]oxazole (14): DABCO (2 mmol) was added to the stirred solution of 1-(2,2-dibromovinyl)-4-methoxybenzene (1 mmol) and 2-amino-4-nitrophenol (1 mmol) in NMP (5 mL) under nitrogen atmosphere. The solution was stirred well for 24 h at 100 °C. After completion, reaction was quenched by the addition of water and extracted with ethyl acetate. The organic layer was washed with brine and dried using MgSO₄, filtered and concentrated under reduced pressure. The crude product was purified using column chromatography. Yellow solid (171 mg, 60%), ¹H NMR (CDCl₃) 8.57–8.56 (m, 1H, CH), 8.28–8.25 (m, 1H, CH), 7.57–7.55 (m, 1H, CH), 7.31–7.29 (m, 2H, 2×CH), 6.91–6.89 (m, 2H, 2×CH), 4.66 (s, 2H, -CH₂-), 3.80 (s, 3H, -OCH₃).

(S)-2-(2,3-dichlorophenoxy)-N-(2-(4-methoxybenzyl)benzo[d]oxazol-5-yl)propanamide (15): 5-Nitro-2-arylbenzo[d]oxazoles (1 mmol) was dissolved in 10 mL EtOAc:MeOH (1:1) and 10% Pd/C (catalytic) was added and stirred well under a H₂ atmosphere for 2–3 h. After the successful completion, reaction mixture was filtered through celite and the filtrate was concentrated under reduced pressure. The crude amine was recrystallized using ethyl acetate and hexane. The amine was proceeded to next step without any chromatographic purification. EDC·HCl (1.5 mmol) was added to the stirred solution of acid **7** (R = 2,3-diCl, 1 mmol), amine (1 mmol) in dry DMF at 0 °C under nitrogen atmosphere. Reaction mixture was stirred well for overnight at room temperature. After completion of the reaction, excess water was added and extracted with ethyl acetate. The organic layer was washed with brine and dried using MgSO₄. The solvent was removed under reduced pressure and crude residue was purified through column chromatography using ethyl acetate/n-hexane. White solid (315 mg, 67%), ¹H NMR (CDCl₃) 8.71 (s, 1H, NH), 7.97 (bs, 1H, CH), 7.46 (d, *J* = 8.00 Hz, 1H, CH), 7.39 (d, *J* = 8.20 Hz, 1H, CH), 7.28 (d, *J* = 8.00 Hz, 2H, 2×CH), 7.18–7.16 (m, 2H, 2×CH), 6.91–6.86 (m, 3H, 3×CH), 4.86 (q, *J* = 6.80 Hz, 1H, CH), 4.19 (s, 2H, -CH₂-), 3.78 (s, 3H, -OCH₃), 1.73 (d, *J* = 7.20 Hz, 3H, CH₃). Purity 97% (t_R = 14.78). m.p. 143–147 C.

Synthesis of 17: A mixture of L-alanine (163 mg, 1.82 mmol), Cs₂CO₃ (1.19 g, 3.65 mmol), and CuI (69.7 mg, 0.36 mmol) was added to the stirred solution of 1,2-dichloro-3-iodobenzene or 1,2-difluoro-3-iodobenzene (1.83 mmol) in dry DMF (3 mL) under a nitrogen atmosphere. The reaction mixture was heated at 90 °C for 24 h. After completion, the reaction mixture was allowed to cool and water was added. The pH was adjusted to 3–5 by the addition of 2N HCl and extracted with ethyl acetate. The organic layer was washed with brine, dried over anhydrous MgSO₄, filtered and concentrated under reduced pressure. The crude acid **16** was used in the next step without further purification. Acid **16** (1 mmol) was added to the stirred solution of amine **5** (Ar = 4-CNPh, 1 mmol) in dry DMF at 0 °C followed by HATU (1.2 mmol) and stirred well for overnight at room temperature. After completion, excess water was added to the reaction and extracted with ethyl acetate. The organic layer was washed with brine and dried over anhydrous MgSO₄, filtered, and concentrated. The residue was purified by column chromatography using ethyl acetate/n-hexane.

(S)-N-(2-(4-Cyanophenyl)benzo[d]oxazol-5-yl)-2-((2,3-dichlorophenyl)amino)propanamide (17a): Light brown powder (202 mg, 45%), ¹H NMR (DMSO-*d*₆) 10.39 (s, 1H, NH), 8.34 (d, *J* = 8.00 Hz, 2H, 2×CH), 8.20 (s, 1H, CH), 8.07 (d, *J* = 8.40 Hz, 2H, 2×CH), 7.81 (d, *J* = 8.40 Hz, 1H, CH), 7.60–7.58 (m, 1H, CH), 7.18 (t, *J* = 8.20 Hz, 1H, CH), 6.88 (d, *J* = 7.60 Hz, 1H, CH), 6.65 (d, *J* = 8.40 Hz, 1H, CH), 5.61 (d, *J* = 8.00 Hz, 1H, NH), 4.26 (m, 1H, CH), 1.54 (d, *J* = 6.8 Hz, 3H, CH₃). Purity 99% (t_R = 14.95). m.p. 201–202 C.

(S)-N-(2-(4-Cyanophenyl)benzo[d]oxazol-5-yl)-2-((2,3-difluorophenyl)amino)propanamide (17b): Yellow powder (225 mg, 54%) ¹H NMR (DMSO-*d*₆) 10.29 (s, 1H, NH), 8.33 (d, *J* = 8.40 Hz, 2H, 2×CH), 8.20 (m, 1H, CH), 8.07 (d, *J* = 8.40 Hz, 1H, CH), 7.77 (d, *J* = 8.80 Hz, 1H, CH), 7.60 (d, *J* = 8.80 Hz, 1H, CH), 6.96 (q, *J* = 7.60 Hz, 1H, CH), 6.59 (m, 1H, CH), 6.51 (t, *J* = 7.60 Hz, 1H, CH), 5.92 (d, *J* = 7.60 Hz, 1H, NH), 4.18 (q, *J* = 6.80 Hz, 1H, CH), 1.51 (d, *J* = 6.40 Hz, 3H, CH₃). Purity 99% (t_R = 12.95). m.p. 197–198 C.

Synthesis of 18: Arylbenzoxazole **8i** or **8j** (1 mmol) was dissolved in dry DMF (5 mL) in an oven dried round bottom flask and cooled to 0 °C. K₂CO₃ (2 mmol) was added to the cold solution and stirred well for ten minutes, then ethyl bromoacetate (1.5 mmol) was added and stirred well at room temperature for 6 h. After completion, the reaction was quenched with water and extracted with ethyl acetate (20 mL) and the organic layer was washed with brine. The organic layer was dried using anhydrous MgSO₄, filtered and concentrated under reduced pressure. The crude residue was purified through column chromatography using hexane: ethyl acetate.

Ethyl (S)-2-(4-(5-(2-(2,3-dichlorophenoxy)propanamido)benzo[d]oxazol-2-yl)phenoxy)acetate (18a): White powder (438 mg, 83%), ¹H NMR (DMSO-*d*₆) 10.31 (s, 1H, NH), 8.08–8.03 (m, 3H, 3×CH), 7.66–7.64 (m, 1H, CH), 7.50–7.48 (m, 1H, CH), 7.29–6.98 (m, 5H, 5×CH), 4.97 (q, *J* = 6.40 Hz, 1H, CH), 4.87 (s, 2H, -OCH₂-), 4.13 (q, *J* = 7.20

Hz, 2H, -OCH₂-), 1.58 (d, *J* = 6.80 Hz, 3H, CH₃), 1.17 (t, *J* = 7.20 Hz, 3H, CH₃). Purity 99% (*t_R* = 15.02). m.p. 144–145 C.

Ethyl(S)-2-(3-(5-(2-(2,3-dichlorophenoxy)propanamido)benzo[d]oxazol-2-yl)phenoxy)acetate (18b): White powder (422 mg, 80%), ¹H NMR (DMSO-*d*₆) 10.35 (s, 1H, NH), 8.09 (m, 1H, CH), 7.76 (d, *J* = 8.00 Hz, 1H, CH), 7.70 (d, *J* = 8.00 Hz, 1H, CH), 7.62–7.61 (m, 1H, CH), 7.55–7.47 (m, 2H, 2×CH), 7.27 (t, *J* = 6.20 Hz, 1H, CH), 7.21–7.18 (m, 2H, 2×CH), 7.02–7.00 (m, 1H, CH), 4.98 (q, *J* = 6.80 Hz, 1H, CH), 4.89 (s, 2H, -OCH₂-), 4.15 (q, *J* = 7.20 Hz, 2H, -OCH₂-), 1.59 (d, *J* = 6.40 Hz, 3H, CH₃), 1.18 (t, *J* = 6.80 Hz, 3H, CH₃). Purity 99% (*t_R* = 13.28). m.p. 175–176 C.

Synthesis of 19: The ester **18** was subjected to ester hydrolysis using the general procedure described for **7**.

(S)-2-(4-(5-(2-(2,3-Dichlorophenoxy)propanamido)benzo[d]oxazol-2-yl)phenoxy)acetic acid (19a): White powder (440 mg, 88%), ¹H NMR (DMSO-*d*₆) 10.36 (s, 1H, NH), 8.12 (d, *J* = 8.80 Hz, 2H, 2×CH), 8.08 (m, 1H, CH), 7.70 (d, *J* = 8.80 Hz, 1H, CH), 7.50 (m, 1H, CH), 7.32 (t, *J* = 8.40 Hz, 1H, CH), 7.25 (m, 1H), 7.13 (d, *J* = 8.80 Hz, 2H, 2×CH), 7.05 (d, *J* = 8.00 Hz, 1H, CH), 5.02 (q, *J* = 6.40 Hz, 1H, CH), 4.82 (s, 2H, -OCH₂-), 1.63 (d, *J* = 6.40 Hz, 3H, CH₃). Purity 98% (*t_R* = 12.64). m.p. 238–239 C.

(S)-2-(3-(5-(2-(2,3-Dichlorophenoxy)propanamido)benzo[d]oxazol-2-yl)phenoxy)acetic acid (19b): White powder (430 mg, 86%), ¹H NMR (DMSO-*d*₆) 13.07 (bs, 1H, COOH), 10.35 (s, 1H, NH), 8.09 (m, 1H, CH), 7.76–7.70 (m, 2H, 2×CH), 7.59–7.46 (m, 3H, 3×CH), 7.26 (t, *J* = 8.00 Hz, 1H, CH), 7.21–7.14 (m, 2H, 2×CH), 7.01 (d, *J* = 8.00 Hz, 1H, CH), 4.98 (q, *J* = 6.40 Hz, 1H, CH), 4.79 (s, 2H, -OCH₂-), 1.59 (d, *J* = 6.40 Hz, 3H, CH₃). Purity 97% (*t_R* = 12.77). m.p. 191–dec C.

Prop-2-yn-1-yl (S)-2-(4-(5-(2-(2,3-dichlorophenoxy)propanamido)benzo[d]oxazol-2-yl)phenoxy)acetate (20): Arylbenzoxazole **19a** (1 mmol) was dissolved in dry DMF (5 mL) in an oven dried round bottom flask and cooled to 0 °C. K₂CO₃ (2 mmol) was added to the cold solution and stirred well for ten minutes, followed by propargyl bromide 80% solution in toluene (1.5 mmol) was added and stirred well at room temperature for 6 h. After completion, reaction was quenched with water and extracted with ethyl acetate (20 mL) and organic layer was washed with brine. The organic layer was dried using MgSO₄, filtered and concentrated under reduced pressure. The crude product was purified through column chromatography. White solid (435 mg, 81%), ¹H NMR (DMSO-*d*₆) 10.37 (s, 1H, NH), 8.12 (d, *J* = 8.80 Hz, CH, 2×CH), 8.08 (m, 1H, CH), 7.72–7.70 (d, *J* = 8.80 Hz, 1H, CH), 7.55 (d, *J* = 8.00 Hz, 1H, CH), 7.34–7.26 (m, 2H, 2×CH), 7.17 (d, *J* = 8.40 Hz, 2H, 2×CH), 7.05 (d, *J* = 8.00 Hz, 1H, CH), 5.03–5.00 (m and s, 3H, CH, -OCH₂-), 4.83 (s, 2H, -OCH₂-), 3.64 (bs, 1H, CH), 1.63 (d, *J* = 6.00 Hz, 3H, CH₃). Purity 98% (*t_R* = 14.69). m.p. 132–133 C.

(S)-4-(5-(2-(2,3-Dichlorophenoxy)propanamido)benzo[d]oxazol-2-yl)-*N*-hydroxybenzamide (21): The ester **8h** (1 mmol) was dissolved in methanol and hydroxylamine hydrochloride (2 mmol) was added at 0 °C and stirred well. KOH (3 mmol)

was added to the cold solution and stirred overnight at room temperature. After completion, the solvent was removed under reduced pressure and the residue was dissolved in water and extracted with ethyl acetate. The organic layer was washed with brine and dried using anhydrous MgSO₄. Solvent was removed under reduced pressure and the product was purified using column chromatography. White powder (310 mg, 65%), ¹H NMR (DMSO-*d*₆) 13.29 (bs, 1H, -OH), 10.37 (s, 1H, NH), 8.26 (d, *J* = 8.00 Hz, 2H, 2×CH), 8.11 (t, *J* = 8.40 Hz, 3H, 3×CH), 7.74 (d, *J* = 9.20 Hz, 1H, CH), 7.56 (d, *J* = 8.80 Hz, 1H, CH), 7.26 (t, *J* = 8.00 Hz, 1H, CH), 7.20 (m, 1H, CH), 7.00 (d, *J* = 8.00 Hz, 1H, CH), 4.99 (q, *J* = 6.80 Hz, 1H, CH), 1.59 (d, *J* = 6.80 Hz, 3H, CH₃). Purity 98% (*t*_R = 13.37). m.p. 253–254 C.

(S)-4-(5-(2-(2,3-Dichlorophenoxy)propanamido)benzo[d]oxazol-2-yl)benzoic acid (22): Ester **8h** (1 mmol) was dissolved in THF:MeOH:H₂O (3:1:1) at room temperature and NaOH (1 mmol) was added and stirred well for 2 h. After completion, the solvents were removed under reduced pressure. The crude residue was dissolved in water and pH was adjusted to 3–5 by the addition of 2N HCl and extracted with ethyl acetate. The organic layer was washed with brine and dried using anhydrous MgSO₄. The crude acid was recrystallized using ethyl acetate and hexane. White powder (423 mg, 90%), ¹H NMR (DMSO-*d*₆) 10.43 (s, 1H, NH), 8.30 (d, *J* = 8.40 Hz, 2H, 2×CH), 8.15 (t, *J* = 9.00, 3H, 3×CH), 7.79 (d, *J* = 8.80 Hz, 1H, CH), 7.61 (d, *J* = 8.80 Hz, 1H, CH), 7.32 (t, *J* = 8.20 Hz, 1H, 1×CH), 7.26–7.24 (m, 1H, CH), 7.05 (d, *J* = 8.00 Hz, 1H, CH), 5.04 (q, *J* = 6.80 Hz, 1H, CH), 1.64 (d, *J* = 6.40 Hz, 3H, CH₃). Purity 98% (*t*_R = 13.33). m.p. 244 C.

(S)-2-(2,3-Dichlorophenoxy)-N-(2-(4-(hydrazinecarbonyl)phenyl)benzo[d]oxazol-5-yl)propanamide (23): Hydrazine hydrate (3 mmol) was added to the stirred solution of **8h** (1 mmol) in ethanol (10 mL) at room temperature and refluxed for 5 h. After completion, the solvent was removed under reduced pressure, water was added and extracted with ethyl acetate. The organic layer was washed with brine and dried using anhydrous MgSO₄. The solvent was removed under reduced pressure and the crude mixture was purified through column chromatography. White powder (324 mg, 67%), ¹H NMR (DMSO-*d*₆) 10.41 (s, 1H, NH), 9.97 (s, 1H, NH), 8.25 (d, *J* = 6.80 Hz, 2H, 2×CH), 8.16 (m, 1H, CH), 8.03 (d, *J* = 6.80 Hz, 2H, 2×CH), 7.77 (d, *J* = 9.2 Hz, 1H, CH), 7.60 (d, *J* = 8.40 Hz, 1H, CH), 7.32 (t, *J* = 7.60, 1H, CH), 7.25 (m, 1H), 7.05 (d, *J* = 8.40 Hz, 1H, CH), 5.03 (q, *J* = 6.80 Hz, 1H, CH), 4.60 (bs, 2H, NH₂), 1.58 (d, *J* = 6.80 Hz, 3H, CH₃). Purity 97% (*t*_R = 10.37). m.p. 247–248 C.

(S)-2-(2,3-Dichlorophenoxy)-N-(2-(4-(5-oxo-4,5-dihydro-1,3,4-oxadiazol-2-yl)phenyl)benzo[d]oxazol-5-yl)propanamide (24): To the stirred solution of **23** (1 mmol) in anhydrous DMF (2 mL), carbonyldiimidazole (1.2 mmol) and diisopropylethylamine (1.2 mmol) was added. The reaction mixture was stirred for 2 h at room temperature. The reaction mixture was diluted with water and extracted with ethyl acetate. The combined extract was washed with brine, dried using anhydrous MgSO₄, filtered and concentrated. The residue was purified through column chromatography (2–8% MeOH gradient in CH₂Cl₂) to give the title compound. White solid (336 mg, 66%), ¹H NMR (DMSO-*d*₆) 12.78 (s, 1H, NH), 10.44 (s, 1H, NH), 8.33 (d, *J* = 7.60 Hz, 2H, 2×CH), 8.17 (m, 1H, CH), 8.01 (d, *J* = 8.00 Hz, 2H, 2×CH), 7.78 (d, *J* = 5.20 Hz, 1H, CH), 7.61 (d, *J*

= 8.80 Hz, 1H, CH), 7.32 (t, J = 8.40 Hz, 1H, CH), 7.25 (m, 1H, CH), 7.06 (d, J = 8.00 Hz, 1H, CH), 5.04 (q, J = 6.80 Hz, 1H, CH), 1.64 (d, J = 6.00 Hz, 3H, CH₃). Purity 99% (t_R = 13.05). m.p. 288-dec C.

(S,Z)-2-(2,3-Dichlorophenoxy)-N-(2-(4-(N'-hydroxycarbamimidoyl)phenyl)benzo[d]oxazol-5-yl)propanamide (25): (*S*)-*N*-(2-(4-cyanophenyl)benzo[d]oxazol-5-yl)-2-(2,3-dichlorophenoxy)propanamide **8f** (1 mmol) was dissolved in anhydrous ethanol (5 mL) followed by hydroxylamine hydrochloride (3 mmol) and triethylamine (6 mmol) was added. The reaction mixture was refluxed for 4 h and the solvent was removed under reduced pressure. The residue was suspended in water and extracted with DCM (20 mL). Organic layer was washed with brine and dried using anhydrous MgSO₄. The solvent was removed under reduced pressure and the crude product was purified through column chromatography (2–8% MeOH gradient in CH₂Cl₂) to give the title compound. White solid (396 mg, 82%), ¹H NMR (DMSO-*d*₆) 10.34 (s, 1H, NH), 9.85 (s, 1H, OH), 8.13–8.08 (m, 2H, 2×CH), 7.86–7.84 (m, 2H, 2×CH), 7.71–7.68 (m, 1H, CH), 7.53–7.51 (m, 1H, CH), 7.28–7.18 (m, 3H, 3×CH), 7.00–6.98 (m, 1H, CH), 5.90 (s, 2H, NH₂), 4.97 (m, 1H, CH), 1.57 (m, 3H, CH₃). Purity 97% (t_R = 14.97). m.p. 196–197 C.

(S)-2-(2,3-Dichlorophenoxy)-N-(2-(4-(5-oxo-4,5-dihydro-1,2,4-oxadiazol-3-yl)phenyl)benzo[d]oxazol-5-yl)propanamide (26): To the stirred solution of **25** (1 mmol) in anhydrous DMF (2 mL), carbonyldiimidazole (1.2 mmol) and diisopropylethylamine (1.2 mmol) was added. The reaction mixture was stirred for 2 h at room temperature. The reaction mixture was diluted with water and extracted with ethyl acetate. The combined extract was washed with brine, dried using anhydrous MgSO₄, filtered and concentrated. The residue was purified through column chromatography (2–8% MeOH gradient in CH₂Cl₂) to give the title compound. White solid (321 mg, 61%), ¹H NMR (DMSO-*d*₆) 10.49 (s, 1H, NH), 9.60 (bs, 1H, NH), 8.32 (d, J = 8.40 Hz, 2H, 2×CH), 8.15 (m, 1H, CH), 7.99 (d, J = 8.40 Hz, 2H, 2×CH), 7.72 (m, 1H, CH), 7.58 (m, 1H, CH), 7.27 (t, J = 7.60 Hz, 1H, CH), 7.21 (m, 1H, CH), 7.02 (d, J = 8.40 Hz, 1H, CH), 5.03 (q, J = 6.80 Hz, 1H, CH), 1.59 (d, J = 6.80 Hz, 3H, CH₃). Purity 98% (t_R = 13.04). m.p. 260 C.

(S)-N-(2-(4-(1H-Tetrazol-5-yl)phenyl)benzo[d]oxazol-5-yl)-2-(2,3-dichlorophenoxy)propanamide (27): A mixture of (*S*)-*N*-(2-(4-cyanophenyl)benzo[d]oxazol-5-yl)-2-(2,3-dichlorophenoxy)propanamide **8f** (1 mmol), NaN₃ (2 mmol), and NH₄Cl (2 mmol) in DMF (1.5 mL) was heated at 100 °C for 6 h. Solvent was removed under reduced pressure, water was added and extracted with ethyl acetate. The organic layer was washed with brine, dried using anhydrous MgSO₄, filtered and concentrated under reduced pressure. The crude residue was purified through column chromatography. White solid (306 mg, 62%), ¹H NMR (DMSO-*d*₆) 11.11 (s, 1H, NH), 10.38 (s, 1H, NH), 8.36–8.34 (m, 1H, CH), 8.22 (d, J = 5.80 Hz, 2H, 2×CH), 8.13 (m, 1H, CH), 7.90 (m, 1H, CH), 7.76–7.70 (m, 1H, CH), 7.59–7.50 (m, 1H, CH), 7.30–7.21 (m, 2H, 2×CH), 7.00 (m, 1H, CH), 5.01 (m, 1H, CH), 1.59 (m, 3H, CH₃). Purity 99% (t_R = 12.25). m.p. 257 C.

(S)-4-(5-(2-(2,3-Dichlorophenoxy)propanamido)benzo[d]oxazol-2-yl)benzamide (28): To the stirred solution of (*S*)-*N*-(2-(4-cyanophenyl)benzo[d]oxazol-5-yl)-2-(2,3-dichlorophenoxy)prop-anamide **8f** (1 mmol) in dry tert-butyl alcohol (4 mL/mmol), KOtBu (3 mmol), was added. The reaction mixture was stirred at room temperature for 12 h under a nitrogen atmosphere, and progress of the reaction was monitored by TLC. Upon completion, the reaction mixture was quenched with water and extracted with ethyl acetate. The organic layer was washed with brine, dried using anhydrous MgSO₄ and solvent was removed under reduced pressure. The crude mixture was purified through column chromatography. White solid (253 mg, 54%), ¹H NMR (DMSO-*d*₆) 10.36 (s, 1H, NH), 8.21 (d, *J* = 8.00 Hz, 2H, 2×CH), 8.12 (s, 2H, NH₂), 8.03 (d, *J* = 8.00 Hz, 2H, 2×CH), 7.73 (d, *J* = 8.40 Hz, 1H, CH), 7.55 (d, *J* = 8.40 Hz, 1H, CH), 7.51 (m, 1H, CH), 7.26 (t, *J* = 8.00 Hz, 1H, CH), 7.20 (m, 1H), 7.00 (d, *J* = 8.40 Hz, 1H, CH) 4.98 (q, *J* = 6.80 Hz, 1H, CH), 1.59 (d, *J* = 6.80 Hz, 3H, CH₃). Purity 98% (t_R = 11.56). m.p. 232 C.

(S)-N-(2-(4-(Aminomethyl)phenyl)benzo[d]oxazol-5-yl)-2-(2,3-dichlorophenoxy)propanamide (29): To a stirred solution of (*S*)-*N*-(2-(4-cyanophenyl)benzo[d]oxazol-5-yl)-2-(2,3-dichlorophenoxy)propanamide **8f** (2.0 mmol) in THF: MeOH (15 mL), Boc₂O (873 mg, 4.0 mmol) and NiCl₂·6H₂O (48 mg, 0.2 mmol) were added at 0 °C and stirred for five minutes. After five minutes, NaBH₄ (530 mg, 14.0 mmol) was added in small portions over 30 min followed by stirring at room temperature for 2h. The reaction mixture was filtered through celite and the filtrate was concentrated under reduced pressure. The crude residue was poured into 1N HCl and extracted with ethyl acetate. The organic layer was washed with brine and dried using anhydrous MgSO₄. Solvent was removed under reduced pressure and crude reaction mixture was purified through column chromatography. Trifluoroacetic acid (1 mL) was added to the stirred solution of Boc protected amine (1 mmol) in dry DCM (5 mL) at 0 °C. After 4 h, the reaction was quenched with a saturated NaHCO₃ solution and extracted with DCM. The organic layer was washed with brine and dried using anhydrous MgSO₄. The solvent was removed under reduced pressure and the product was recrystallized using ethyl acetate and hexane. White solid (305 mg, 67%), ¹H NMR (DMSO-*d*₆) 10.40 (s, 1H, NH), 8.14–8.10 (m, 3H, 3×CH), 7.73 (d, *J* = 9.20 Hz, 1H, CH), 7.58–7.56 (m, 3H, 3×CH), 7.32 (t, *J* = 8.20 Hz, 1H, CH), 7.26–7.24 (m, 1H, CH), 7.05 (d, *J* = 8.00 Hz, 1H, CH), 5.03 (q, *J* = 6.80 Hz, 1H, CH), 3.82 (s, 3H, -OCH₃), 1.64–1.63 (d, *J* = 6.00 Hz, 3H, CH₃). Purity 97% (t_R = 14.63). m.p. 189-dec C.

(S)-2-(2,3-Dichlorophenoxy)-N-(2-(2-oxo-1,2-dihydropyridin-4-yl)benzo[d]oxazol-5-yl)propanamide (30): To the stirred solution of **8b** (1 mmol) in DMF, LiCl (5 mmol) and p-TSA (5 mmol) was added and stirred well for 2 h at 120 °C. After completion, reaction was quenched with saturated NaHCO₃ solution and extracted with ethyl acetate. The organic layer was washed with brine and dried using MgSO₄. Solvent was removed under reduced pressure and crude residue was purified through column chromatography. White solid (341 mg, 77%), ¹H NMR (DMSO-*d*₆) 12.20 (bs, 1H, NH), 10.30 (s, 1H, NH), 8.19 (s, 1H, CH), 8.02 (dd, *J* = 9.80 Hz, *J* = 2.20 Hz, 1H, CH), 7.98 (m, 1H, CH), 7.61 (d, *J* = 9.20 Hz, 1H, CH), 7.46 (m, 1H, CH), 7.27 (t, *J* = 8.00 Hz, 1H, CH),

7.19 (m, 1H), 6.99 (d, $J = 8.80$ Hz, 1H, CH), 6.47 (d, $J = 9.60$ Hz, 1H, CH), 4.97 (q, $J = 6.40$ Hz, 1H, CH), 1.58 (d, $J = 6.80$ Hz, 3H, CH₃). Purity 97% ($t_R = 10.25$). m.p. 240–241 C.

(S)-4-(5-(2-(2,3-Dichlorophenoxy)propanamido)benzo[d]oxazol-2-yl)pyridine-1-oxide (31): *m*-Chloroperoxybenzoic acid (2 mmol) was added to the stirred solution of **8a** (1 mmol) in dry DCM at rt and stirred well for overnight. After completion, reaction was quenched with saturated NaHCO₃ solution and extracted with DCM. The organic layer was washed with brine, dried using MgSO₄, filtered and concentrated under reduced pressure. The crude product was purified through column chromatography. White solid (327 mg, 74%), ¹H NMR (DMSO-*d*₆) 10.43 (s, 1H, NH), 8.38 (d, $J = 6.80$ Hz, 2H, 2×CH), 8.17 (m, 1H, CH), 8.09 (d, $J = 6.80$ Hz, 2H, 2×CH), 7.78–7.76 (m, 1H, CH), 7.63–7.60 (m, 1H, CH), 7.16–7.12 (m, 1H, CH), 7.06–7.02 (m, 1H, CH), 6.95–6.92 (m, 1H, CH), 5.00 (q, $J = 6.80$ Hz, 1H, CH), 1.62 (d, $J = 6.80$ Hz, 3H, CH₃). Purity 99% ($t_R = 10.80$). m.p. 125-dec C.

(S)-2-(2-(Aminomethyl)phenoxy)-N-(2-(4-methoxyphenyl)benzo[d]oxazol-5-yl)propanamide (32): The reaction was proceeded with **8u** using the procedure, which used for the synthesis of **29**. White solid (283 mg, 68%), ¹H NMR (DMSO-*d*₆) 11.10 (bs, 1H, NH), 8.13–8.11 (d, $J = 9.2$ Hz, 2H, 2×CH), 8.02–8.01 (m, 1H, CH), 7.67 (d, $J = 8.2$ Hz, 1H, CH), 7.54–7.51 (m, 1H, CH), 7.29–7.14 (m, 3H, 3×CH), 7.04–7.02 (m, 1H, CH), 6.93–6.91 (m, 1H, CH), 5.06 (q, $J = 6.80$ Hz, 1H, CH), 3.71 (s, 3H, -OCH₃), 1.62 (d, $J = 6.80$ Hz, 3H, CH₃). Purity 97% ($t_R = 14.31$). m.p. 160–161 C.

(S)-N-(2-(4-Cyanophenyl)benzo[d]oxazol-5-yl)-2-(2-hydroxyphenoxy)propanamide (33): Compound **8v** (1 mmol) was dissolved in 10 mL EtOAc: MeOH (1:1) and 10% Pd/C (catalytic) was added and stirred well under a H₂ atmosphere for 3 h. After the successful completion, reaction mixture was filtered through celite and the filtrate was concentrated under reduced pressure. The crude product was purified through column chromatography. White solid (359 mg, 90%), ¹H NMR (DMSO-*d*₆) 10.26 (s, 1H, NH), 9.29 (s, 1H, OH), 8.34 (d, $J = 8.4$ Hz, 2H, 2×CH), 8.22–8.21 (m, 1H, CH), 8.08 (d, $J = 8.80$ Hz, 2H, 2×CH), 7.81 (d, $J = 8.80$ Hz, 1H, CH), 7.68–7.66 (m, 1H, CH), 7.05–7.03 (d, $J = 7.6$ Hz, 1H, CH), 6.88–6.83 (m, 2H, 2×CH), 6.71–6.73 (m, 1H, CH), 4.87 (q, $J = 6.80$ Hz, 1H, CH), 1.57 (d, $J = 6.80$ Hz, 3H, CH₃). Purity 99% ($t_R = 11.10$). m.p. 185–186 C.

Methyl (S)-2-(2-bromo-3-formylphenoxy)propanoate (34): 2-Bromo-3-hydroxybenzaldehyde (1 mmol) was added to the solution of (+)-methyl-D-lactate (1.38 mmol) in anhydrous THF (6 mL) under a nitrogen atmosphere and the solution was cooled to 0 °C. PPh₃ (1.20 mmol) was added portion wise and stirred for 10 min followed by the dropwise addition of DEAD (1.50 mmol) over 20 min. The reaction mixture was stirred for 2 h at room temperature. After completion, the solvent was removed under reduced pressure and the crude mixture was purified through column chromatography using ethyl acetate/n-hexane (10:90) to yield methyl ((S)-2-(2-bromo-3-formylphenoxy)propanoate (236 mg, 83%) as a white solid.

Methyl (S)-2-(2-bromo-3-((methoxymethoxy)methyl)phenoxy)propanoate (35): Under a nitrogen atmosphere, NaBH₄ (1.5 mmol) was added to the stirred solution of

((S)-2-(2-bromo-3-formylphenoxy)propanoate **34** (1 mmol) in ethanol at 0 °C. After 1 h at room temperature, the reaction was quenched with a saturated NaHCO₃ solution and extracted with ethyl acetate. The organic layer was washed with brine and dried using anhydrous MgSO₄, filtered and concentrated under reduced pressure. The crude product was dissolved in dry DCM and cooled to 0 °C. DIPEA (5 mmol) was added, followed by dropwise addition of MOMCl (3 mmol) and stirred for overnight at room temperature. After completion, the reaction was quenched with saturated NH₄Cl and extracted with DCM. The organic layer was dried using anhydrous MgSO₄ and the solvent was removed under reduced pressure. The crude residue was purified through column chromatography. White solid (239 mg, 72%), ¹H NMR (DMSO-*d*₆) 7.32–7.28 (m, 1H, CH), 7.12–7.09 (m, 1H, CH), 6.90–6.88 (m, 1H, CH), 5.06 (m, 1H, CH), 4.70 (bs, 3H, -OCH₃), 4.61–4.51 (m, 4H, 2×-OCH₂-), 3.68 (s, 3H, -COOCH₃), 1.55 (m, 3H, CH₃).

Methyl (S)-2-(3-((methoxymethoxy)methyl)-2-(4,4,5,5-tetramethyl-1,3,2-dioxaborolan-2-yl)phenoxy)propanoate (36): To a solution of methyl (S)-2-(2-bromo-3-((methoxymethoxy)methyl)phenoxy)propanoate **35** (400 mg, 1.145 mmol) in 1,4-dioxane (6 mL) was added KOAc (483 mg, 4.923 mmol), Pin₂B₂ (349 mg, 1.37 mmol) and Pd(Ph₃P)₂Cl₂ (80 mg, 0.114 mmol) under an argon atmosphere. The reaction flask was placed under vacuum and then backfilled with argon (two times). Then the reaction was stirred at 95 °C for overnight. The solvent was removed under reduced pressure and the residue was suspended in water and extracted with ethyl acetate. The organic layer was washed with brine and dried over anhydrous MgSO₄, filtered and concentrated. The crude product was purified through column chromatography using hexane/ethyl acetate. White solid (243 mg, 64%), ¹H NMR (DMSO-*d*₆) 7.28–7.24 (m, 1H, CH), 6.93–6.88 (m, 1H, CH), 6.68–6.66 (m, 1H, CH), 4.90–4.86 (m, 1H, CH), 4.56 (bs, 4H, 2×-OCH₂-), 4.47 (bs, 3H, -OCH₃), 3.67 (s, 3H, -COOCH₃), 1.45 (m, 3H, CH₃), 1.29 (bs, 12H, 4×CH₃).

(S)-N-(2-(4-Cyanophenyl)benzo[d]oxazol-5-yl)-2-((1-hydroxy-1,3-dihydrobenzo[c][1,2]oxaborol-7-yl)oxy)propanamide (37): Ester **36** (1 mmol) was dissolved in 5 mL THF: MeOH (2:3) and stirred at 0 °C. LiOH (1.5 mmol) was added portion wise to the solution and stirred well at room temperature for 4 h. The solvents were removed under reduced pressure, crude residue was dissolved in ethyl acetate and 1N HCl was added until a pH of 4 was reached. The product was extracted with ethyl acetate and the organic extracts were combined, washed with brine, dried over anhydrous MgSO₄. The solvent was removed under reduced pressure and crude acid was used in the next step without chromatographic purification. EDC·HCl (1.5 mmol) was added to the stirred solution of acid (1 mmol), amine **5** (Ar = 4-CNPh, 1 mmol) in dry DMF at 0 °C under nitrogen atmosphere. Reaction mixture was stirred well for overnight at room temperature. After completion of the reaction, excess water was added and extracted with ethyl acetate. The organic layer was washed with brine and dried using MgSO₄. The solvent was removed under reduced pressure. The crude residue was purified through column chromatography give desired coupled product. To a solution of this MOM protected material (140 mg, 0.363 mmol) in THF (0.9 mL) 4 N HCl (0.43 mL, 18.1 mmol) was added. The reaction was stirred at room temperature for 4 h, upon completion ethyl acetate was added and extracted. The organic phase was washed with brine, dried over anhydrous MgSO₄, filtered and concentrated under reduced pressure. The

crude product was purified through column chromatography using hexane/ethyl acetate. Brown solid (122 mg, 28%). ¹H NMR (DMSO-*d*₆) 10.13 (s, 1H, NH), 9.20 (s, 1H, OH), 8.34 (d, *J* = 8.4 Hz, 2H, 2×CH), 8.22 (m, 1H, CH), 8.08 (d, *J* = 8.40 Hz, 2H, 2×CH), 7.80 (d, *J* = 9.2 Hz, 1H, CH), 7.70 (m, 1H, CH), 7.45 (m, 1H, CH), 7.04 (d, *J* = 7.60 Hz, 1H, CH), 6.93 (d, *J* = 7.60 Hz, 1H, CH), 5.03 (q, *J* = 6.80 Hz, 1H, CH), 4.98 (s, 2H, -OCH₂-), 1.62 (d, *J* = 6.8 Hz, 3H, CH₃). Purity 97% (*t*_R = 11.27). m.p. hygroscopic.

Inhibition of *Mtb*IMPDH.—The $K_{i,app}$ values were determined by measuring the initial velocities at varying concentrations of the inhibitors (1–10,000 nM) with fixed concentrations of IMP (0.5 mM) and NAD⁺ (1.5 mM) and *Mtb*IMPDH2 (20–50 nM). Inhibition of human IMPDH2 was assayed IMP using (0.25 mM) and NAD⁺ (0.060 mM) and *h*IMPDH2 (250 nM). Inhibition of human GMPR2 was assayed using GMP (0.050 mM), NADPH (0.045 mM) and enzyme (100 nM). The assay buffer contained 50 mM TrisCl, pH 8.0, 100 mM KCl and 1 mM dithiothreitol.

The values of $K_{i,app}$ were obtained using the equations (1) and (2)

$$v_i = v_0 / (1 + [I] / IC_{50}) \quad (1)$$

$$K_{i,app} = IC_{50} - [E] / 2 \quad (2)$$

where v_i is the initial velocity in the presence of inhibitor and v_0 is the initial velocity in the absence of the inhibitor. If the IC_{50} value is comparable to the enzyme concentration, the Morrison tight binding equation was used to determine $K_{i,app}$ (3)

$$v_i / v_0 = 1 - \left(\left([E] + [I] + K_{i,app} \right) - \left(\left([E] + [I] + K_{i,app} \right)^2 - 4[E][I] \right)^{0.5} \right) / (2[E]) \quad (3)$$

where [E] is the concentration of the enzyme. All the initial velocity measurements were performed in triplicates. The $K_{i,app}$ values reported are the average of at least two independent experiments unless otherwise noted.

MIC determinations.—MICs were determined as previously described.⁹ MIC values were determined in at least triplicate according to the broth microdilution methods using compounds from DMSO stock solutions. Isoniazid was used as a positive control and DMSO was utilized as a negative control. Isolated *Mtb* cells (ATCC 27294) were cultured to an OD 0.2–0.3 in the required medium, then diluted to deliver approximately 1×10^4 bacteria per well of a 96 well clear round-bottom plate. Plates were read after 1 week with an inverted enlarging mirror plate reader and graded as either growth or no growth. GAST/Fe medium (per liter) consisted of 0.3 g of Bacto Casitone (Difco), 4.0 g of dibasic potassium phosphate, 2.0 g of citric acid, 1.0 g of L-alanine, 1.2 g of magnesium chloride hexahydrate, 0.6 g of potassium sulfate, 2.0 g of ammonium chloride, 1.80 ml of 10 N

sodium hydroxide, and 10.0 ml of glycerol, 0.05% Tween 80 and 0.05 g of ferric ammonium citrate adjusted to pH 6.6. 7H9/glycerol/glucose/BSA/Tween medium consisted of Middlebrook 7H9 broth base supplemented per liter with 0.2% glucose, 0.2% glycerol, 0.5% BSA fraction V, 0.08% NaCl and 0.05% Tween 80. Cultures were supplemented with 200 μ M guanine as noted.

***Mtb* IMPDH2 downregulation and susceptibility of SRMV2.6.**—*Mtb* strains *guaB2* cKD (*guaB2-B3* Tet-OFF *attB::guaB3*) and SRMV2.6, which carries *guaB2*^{Y487C}, were cultured in Middlebrook 7H9 media (Difco) supplemented with 0.2% glycerol, Middlebrook oleic acid-albumin-dextrose-catalase (OADC) enrichment (Difco) and 0.05% Tween 80 (7H9/Glycerol/OADC/Tween). Hygromycin (Hyg), kanamycin (Km) and gentamycin (Gm) were used in *guaB2* cKD culture at final concentrations of 50, 25 and 2.5 μ g/mL, respectively. ATc (Sigma) was used at concentrations up to 100 ng/mL. For pairwise combination (checkerboard) assays, a two-dimensional array of serial dilutions of test compound and ATc was prepared in 96-well plates, as previously described.¹¹ MIC testing was carried out by broth microdilution using the AlamarBlue (AB, Invitrogen) assay^{51, 52}.

Mammalian Cell Culture.—Hep G2 cells (ATCC, purchased February 2017) were cultivated in EMEM supplemented with 10% heat inactivated FBS and 1X penicillin/streptomycin under standard conditions (37 °C in a 5% CO₂ humidified atmosphere). HEK293T, MCF7 and HELA cells were cultured in DMEM with 10% heat inactivated FBS and 1X penicillin/streptomycin. Active cell cultures routinely tested for presence of Mycoplasma (MycAlert™ detection kit, Lonza) and confirmed to be Mycoplasma free.

LDH Cytotoxicity Assay.—All compounds were dissolved in DMSO and further diluted with culture medium before use in tissue culture assays (final DMSO concentrations were 0.1%). To determine cytotoxicity, LDH release was measured with the LDH Cytotoxicity Assay Kit (Pierce) according to manufacturer's protocol. Briefly, 96 well plates were seeded with 13,000 Hep G2 cells (all other cell lines seeded at 6,000 to 8,000 cells per well) and the cells were cultured for 24 h prior to drug treatment. The cells were incubated in 110 μ L of EMEM containing compound or DMSO (vehicle only, control) for 24 h at 37°C. At least four wells from each plate were used as either 'spontaneous' LDH controls or as 'maximum' LDH controls per manufacturer's instructions. Cytotoxicity was determined by measuring absorbance on a microplate reader. Data represent two independent experiments each performed in quadruplicate (n =8).

ADMET studies were performed by GVK Biosciences, (Hyderabad India).

Supplementary Material

Refer to Web version on PubMed Central for supplementary material.

Acknowledgment:

This work was funded with funds from the National Institute of Allergy and Infectious Diseases (NIAID), National Institutes of Health, Department of Health and Human Services (AI093459 to LH, AI125362 to GDC and contracts HHSN272200700058C and HHSN272201200026C to the Center of Structural Genomics of Infectious Diseases);

the Intramural Research Program of NIAID (HB); and the South African Medical Research Council and National Research Foundation (to VM). We thank Xingyou Wang for assistance with the melting points.

Abbreviations Used:

BSA	bovine serum albumin
CBS	cystathione β -synthetase
CDI	carbonyl diimidazole
DCM	dichloromethane
DEAD	diethylazodicarboxylate
DIPEA	diisopropylethylamine
EDC•HCl	1-ethyl-3-(3-dimethylaminopropyl)carbodiimide hydrochloride
EDG	electron donating group
EWG	electron withdrawing group
Gua	guanine
HATU	(1-[bis(dimethylamino)methylene]-1H-1,2,3-triazolo[4,5-b]pyridinium 3-oxid hexafluorophosphate)
IMP	inosine 5'-monophosphate
IMPDH2	inosine 5'-monophosphate dehydrogenase 2
LDH	lactate dehydrogenase
<i>m</i>-CPBA	<i>meta</i> -chloroperoxybenzoic acid
MIC	minimum inhibitory concentration
Mtb	Mycobacterium tuberculosis
NAD	nicotinamide adenine dinucleotide
NMP	N-methyl-2-pyrrolidone
<i>p</i>-TSA	<i>para</i> -toluene sulfonic acid
SAR	structure-activity relationship
TEA	triethylamine
TFA	trifluoroacetic acid
XMP	xanthosine 5'-monophosphate

REFERENCES

1. Bloemberg GV; Keller PM; Stucki D; Trauner A; Borrell S; Latshang T; Coscolla M; Rothe T; Homke R; Ritter C; Feldmann J; Schulthess B; Gagneux S; Bottger EC Acquired resistance to bedaquiline and delamanid in therapy for tuberculosis. *N. Engl. J. Med* 2015, 373, 1986–1988. [PubMed: 26559594]
2. Hedstrom L IMP Dehydrogenase: structure, mechanism and inhibition. *Chem. Rev* 2009, 109, 2903 – 2928. [PubMed: 19480389]
3. Hedstrom L; Liechti G; Goldberg JB; Gollapalli DR The antibiotic potential of prokaryotic IMP dehydrogenase inhibitors. *Curr. Med Chem* 2011, 18, 1909–18. [PubMed: 21517780]
4. Cole ST; Brosch R; Parkhill J; Garnier T; Churcher C; Harris D; Gordon SV; Eiglmeier K; Gas S; Barry CE, 3rd; Tekaia F; Badcock K; Basham D; Brown D; Chillingworth T; Connor R; Davies R; Devlin K; Feltwell T; Gentles S; Hamlin N; Holroyd S; Hornsby T; Jagels K; Krogh A; McLean J; Moule S; Murphy L; Oliver K; Osborne J; Quail MA; Rajandream MA; Rogers J; Rutter S; Seeger K; Skelton J; Squares R; Squares S; Sulston JE; Taylor K; Whitehead S; Barrell BG Deciphering the biology of *Mycobacterium tuberculosis* from the complete genome sequence. *Nature* 1998, 393, 537–544. [PubMed: 9634230]
5. Sassetti CM; Boyd DH; Rubin EJ Genes required for mycobacterial growth defined by high density mutagenesis. *Mol. Microbiol* 2003, 48, 77–84. [PubMed: 12657046]
6. DeJesus MA; Gerrick ER; Xu W; Park SW; Long JE; Boutte CC; Rubin EJ; Schnappinger D; Ehrh S; Fortune SM; Sassetti CM; Ioerger TR Comprehensive essentiality analysis of the *Mycobacterium tuberculosis* genome via saturating transposon mutagenesis. *MBio* 2017, 8, e02133–16. [PubMed: 28096490]
7. Usha V; Gurucha SS; Lovering AL; Lloyd AJ; Papaemmanouil A; Reynolds RC; Besra GS Identification of novel diphenyl urea inhibitors of Mt-GuaB2 active against *Mycobacterium tuberculosis*. *Microbiology* 2011, 157, 290–299. [PubMed: 21081761]
8. Chen L; Wilson DJ; Xu Y; Aldrich CC; Felczak K; Sham YY; Pankiewicz KW Triazole-linked inhibitors of inosine monophosphate dehydrogenase from human and *Mycobacterium tuberculosis*. *J. Med. Chem* 2010, 53, 4768–4778. [PubMed: 20491506]
9. Makowska-Grzyska M; Kim Y; Gorla SK; Wei Y; Mandapati K; Zhang M; Maltseva N; Modi G; Boshoff HI; Gu M; Aldrich C; Cuny GD; Hedstrom L; Joachimiak A *Mycobacterium tuberculosis* IMPDH in complexes with substrates, products and antitubercular compounds. *PLoS One* 2015, 10, e0138976. [PubMed: 26440283]
10. Park Y; Pacitto A; Bayliss T; Cleghorn LA; Wang Z; Hartman T; Arora K; Ioerger TR; Sacchettini J; Rizzi M; Donini S; Blundell TL; Ascher DB; Rhee K; Breda A; Zhou N; Dartois V; Jonnal SR; Via LE; Mizrahi V; Epemolu O; Stojanovski L; Simeons F; Osuna-Cabello M; Ellis L; MacKenzie CJ; Smith AR; Davis SH; Murugesan D; Buchanan KI; Turner PA; Huggett M; Zuccotto F; Rebollo-Lopez MJ; Lafuente-Monasterio MJ; Sanz O; Diaz GS; Lelievre J; Ballell L; Selenski C; Axtman M; Ghidelli-Disse S; Pflaumer H; Bosche M; Drewes G; Freiberg GM; Kurnick MD; Srikumaran M; Kempf DJ; Green SR; Ray PC; Read K; Wyatt P; Barry CE, 3rd; Boshoff HI Essential but not vulnerable: indazole sulfonamides targeting inosine monophosphate dehydrogenase as potential leads against *Mycobacterium tuberculosis*. *ACS Infect. Dis* 2017, 3, 18–33. [PubMed: 27704782]
11. Singh V; Donini S; Pacitto A; Sala C; Hartkoorn RC; Dhar N; Keri G; Ascher DB; Mondesert G; Vocat A; Lupien A; Sommer R; Vermet H; Lagrange S; Buechler J; Warner DF; McKinney JD; Pato J; Cole ST; Blundell TL; Rizzi M; Mizrahi V The inosine monophosphate dehydrogenase, GuaB2, is a vulnerable new bactericidal drug target for tuberculosis. *ACS Infect. Dis* 2017, 3, 5–17. [PubMed: 27726334]
12. Usha V; Hobrath JV; Gurucha SS; Reynolds RC; Besra GS Identification of novel Mt-GuaB2 inhibitor series active against *M. tuberculosis*. *PLoS One* 2012, 7, e33886. [PubMed: 22479467]
13. Cox JA; Mugumbate G; Del Peral LV; Jankute M; Abrahams KA; Jervis P; Jackenkroll S; Perez A; Alemparte C; Esquivias J; Lelievre J; Ramon F; Barros D; Ballell L; Besra GS Novel inhibitors of *Mycobacterium tuberculosis* GuaB2 identified by a target based high-throughput phenotypic screen. *Sci. Rep* 2016, 6, 38986. [PubMed: 27982051]

14. Ignoul S; Eggermont J CBS domains: structure, function, and pathology in human proteins. *Am. J. Physiol. Cell Physiol* 2005, 289, C1369–C1378. [PubMed: 16275737]
15. Nimmegern E; Black J; Futer O; Fulghum JR; Chambers SP; Brummel CL; Raybuck SA; Sintchak MD Biochemical analysis of the modular enzyme inosine monophosphate dehydrogenase. *Protein Expr. Purif* 1999, 17, 282–289. [PubMed: 10545277]
16. Gan L; Petsko GA; Hedstrom L Crystal structure of a ternary complex of *Tritrichomonas foetus* inosine 5'-monophosphate dehydrogenase: NAD⁺ orients the active site loop for catalysis. *Biochemistry* 2002, 41, 13309–13317. [PubMed: 12403633]
17. Makowska-Grzyska M; Kim Y; Maltseva N; Osipiuk J; Gu M; Zhang M; Mandapati K; Gollapalli DR; Gorla SK; Hedstrom L; Joachimiak A A novel cofactor-binding mode in bacterial IMP dehydrogenases explains inhibitor selectivity. *J. Biol. Chem* 2015, 290, 5893–5911. [PubMed: 25572472]
18. Makowska-Grzyska M; Kim Y; Wu R; Wilton R; Gollapalli DR; Wang XK; Zhang R; Jedrzejczak R; Mack JC; Maltseva N; Mulligan R; Binkowski TA; Gornicki P; Kuhn ML; Anderson WF; Hedstrom L; Joachimiak A *Bacillus anthracis* inosine 5'-monophosphate dehydrogenase in action: the first bacterial series of structures of phosphate ion-, substrate-, and product-bound complexes. *Biochemistry* 2012, 51, 6148–6163. [PubMed: 22788966]
19. Alexandre T; Raynal B; Munier-Lehmann H Two classes of bacterial IMPDHs according to their quaternary structures and catalytic properties. *PLoS One* 2015, 10, e0116578. [PubMed: 25706619]
20. Labesse G; Alexandre T; Gelin M; Haouz A; Munier-Lehmann H Crystallographic studies of two variants of *Pseudomonas aeruginosa* IMPDH with impaired allosteric regulation. *Acta Crystallogr. D Biol. Crystallogr* 2015, 71, 1890–1899. [PubMed: 26327379]
21. Labesse G; Alexandre T; Vaupre L; Salard-Arnaud I; Him JL; Raynal B; Bron P; Munier-Lehmann H MgATP regulates allostery and fiber formation in IMPDHs. *Structure* 2013, 21, 975–985. [PubMed: 23643948]
22. Buey RM; Ledesma-Amaro R; Velazquez-Campoy A; Balsera M; Chagoyen M; de Pereda JM; Revuelta JL Guanine nucleotide binding to the Bateman domain mediates the allosteric inhibition of eukaryotic IMP dehydrogenases. *Nat. Commun* 2015, 6, 8923. [PubMed: 26558346]
23. Pimkin M; Markham GD The CBS subdomain of inosine 5'-monophosphate dehydrogenase regulates purine nucleotide turnover. *Mol. Microbiol* 2008, 69, 342–359.
24. Pimkin M; Pimkina J; Markham GD A regulatory role of the Bateman domain of IMP dehydrogenase in adenylate nucleotide biosynthesis. *J. Biol. Chem* 2009, 284, 7960–7969. [PubMed: 19153081]
25. McLean JE; Hamaguchi N; Belenky P; Mortimer SE; Stanton M; Hedstrom L Inosine 5'-monophosphate dehydrogenase binds nucleic acids in vitro and in vivo. *Biochem. J* 2004, 379, 243–251. [PubMed: 14766016]
26. Mortimer SE; Xu D; McGrew D; Hamaguchi N; Lim HC; Bowne SJ; Daiger SP; Hedstrom L IMP Dehydrogenase Type 1 Associates with polyribosomes translating rhodopsin mRNA. *J. Biol. Chem* 2008, 283, 36354–36360. [PubMed: 18974094]
27. Kozhevnikova EN; van der Knaap JA; Pindyurin AV; Ozgur Z; van Ijcken WF; Moshkin YM; Verrijzer CP Metabolic enzyme IMPDH is also a transcription factor regulated by cellular state. *Mol. Cell* 2012, 47, 133–139. [PubMed: 22658723]
28. Butland G; Peregrin-Alvarez JM; Li J; Yang W; Yang X; Canadien V; Starostine A; Richards D; Beattie B; Krogan N; Davey M; Parkinson J; Greenblatt J; Emili A Interaction network containing conserved and essential protein complexes in *Escherichia coli*. *Nature* 2005, 433, 531–537. [PubMed: 15690043]
29. Cherkasov A; Hsing M; Zoraghi R; Foster LJ; See RH; Stoykov N; Jiang J; Kaur S; Lian T; Jackson L; Gong H; Swayze R; Amandoron E; Hormozdiari F; Dao P; Sahinalp C; Santos-Filho O; Axerio-Cilies P; Byler K; McMaster WR; Brunham RC; Finlay BB; Reiner NE Mapping the protein interaction network in methicillin-resistant *Staphylococcus aureus*. *J. Proteome Res* 2011, 10, 1139–1150. [PubMed: 21166474]

30. Housden BE; Muhar M; Gemberling M; Gersbach CA; Stainier DY; Seydoux G; Mohr SE; Zuber J; Perrimon N Loss-of-function genetic tools for animal models: cross-species and cross-platform differences. *Nat. Rev. Genet* 2017, 18, 24–40. [PubMed: 27795562]
31. Hedstrom L The bare essentials of antibiotic target validation. *ACS Infect. Dis* 2017, 3, 2–4. [PubMed: 28081610]
32. Umejiego NN; Gollapalli D; Sharling L; Volftsun A; Lu J; Benjamin NN; Stroupe AH; Riera TV; Striepen B; Hedstrom L Targeting a prokaryotic protein in a eukaryotic pathogen: identification of lead compounds against cryptosporidiosis. *Chem. Biol* 2008, 15, 70–77. [PubMed: 18215774]
33. Maurya SK; Gollapalli DR; Kirubakaran S; Zhang M; Johnson CR; Benjamin NN; Hedstrom L; Cuny GD Triazole inhibitors of *Cryptosporidium parvum* inosine 5'-monophosphate dehydrogenase. *J. Med. Chem* 2009, 52, 4623–4630. [PubMed: 19624136]
34. Sharling L; Liu X; Gollapalli DR; Maurya SK; Hedstrom L; Striepen B A screening pipeline for antiparasitic agents targeting *Cryptosporidium* inosine monophosphate dehydrogenase. *PLoS Negl. Trop. Dis* 2010, 4, e794. [PubMed: 20706578]
35. MacPherson IS; Kirubakaran S; Gorla SK; Riera TV; D'Aquino JA; Zhang M; Cuny GD; Hedstrom L The structural basis of *Cryptosporidium*-specific IMP dehydrogenase inhibitor selectivity. *J. Am. Chem. Soc* 2010, 132, 1230–1231. [PubMed: 20052976]
36. Kirubakaran S; Gorla SK; Sharling L; Zhang M; Liu X; Ray SS; Macpherson IS; Striepen B; Hedstrom L; Cuny GD Structure-activity relationship study of selective benzimidazole-based inhibitors of *Cryptosporidium parvum* IMPDH. *Bioorg. Med. Chem. Lett* 2012, 22, 1985–1988. [PubMed: 22310229]
37. Johnson CR; Gorla SK; Kavitha M; Zhang M; Liu X; Striepen B; Mead JR; Cuny GD; Hedstrom L Phthalazinone inhibitors of inosine-5'-monophosphate dehydrogenase from *Cryptosporidium parvum*. *Bioorg. Med. Chem. Lett* 2013, 23, 1004–1007. [PubMed: 23324406]
38. Gorla SK; Kavitha M; Zhang M; Liu X; Sharling L; Gollapalli DR; Striepen B; Hedstrom L; Cuny GD Selective and potent urea inhibitors of *Cryptosporidium parvum* inosine 5'-monophosphate dehydrogenase. *J. Med. Chem* 2012, 55, 7759–7771. [PubMed: 22950983]
39. Gorla SK; Kavitha M; Zhang M; Chin JE; Liu X; Striepen B; Makowska-Grzyska M; Kim Y; Joachimiak A; Hedstrom L; Cuny GD Optimization of benzoxazole-based inhibitors of *Cryptosporidium parvum* inosine 5'-monophosphate dehydrogenase. *J. Med. Chem* 2013, 56, 4028–4043. [PubMed: 23668331]
40. Sun Z; Khan J; Makowska-Grzyska M; Zhang M; Cho JH; Suebsuwong C; Vo P; Gollapalli DR; Kim Y; Joachimiak A; Hedstrom L; Cuny GD Synthesis, in vitro evaluation and cocrystal structure of 4-oxo-[1]benzopyrano[4,3-c]pyrazole *Cryptosporidium parvum* inosine 5'-monophosphate dehydrogenase (*Cp*IMPDH) inhibitors. *J. Med. Chem* 2014, 57, 10544–10550. [PubMed: 25474504]
41. Mandapati K; Gorla SK; House AL; McKenney ES; Zhang M; Rao SN; Gollapalli DR; Mann BJ; Goldberg JB; Cuny GD; Glomski IJ; Hedstrom L Repurposing *Cryptosporidium* inosine 5'-monophosphate dehydrogenase inhibitors as potential antibacterial agents. *ACS Med. Chem. Lett* 2014, 5, 846–850. [PubMed: 25147601]
42. Gorla SK; Zhang Y; Rabideau MM; Qin A; Chacko S; House AL; Johnson CR; Mandapati K; Bernstein HM; McKenney ES; Boshoff H; Zhang M; Glomski IJ; Goldberg JB; Cuny GD; Mann BJ; Hedstrom L Benzoxazoles, phthalazinones, and arylurea-based compounds with IMPDH-independent antibacterial activity against *Francisella tularensis*. *Antimicrob. Agents Chemother* 2017, 61, e00939–17. [PubMed: 28739786]
43. Hedstrom L IMP dehydrogenase: mechanism of action and inhibition. *Curr. Med. Chem* 1999, 6, 545–560. [PubMed: 10390600]
44. Pettersen EF; Goddard TD; Huang CC; Couch GS; Greenblatt DM; Meng EC; Ferrin TE UCSF Chimera- a visualization system for exploratory research and analysis. *J. Comp. Chem* 2004, 25, 1605–1612. [PubMed: 15264254]
45. Midya GC; Kapat A; Maiti S; Dash J Transition-metal-free hydration of nitriles using potassium tert-butoxide under anhydrous conditions. *J. Org. Chem* 2015, 80, 4148–4151. [PubMed: 25786059]

46. Caddick S; Judd DB; Lewis AK d. K.; Reich, M. T.; Williams, M. R. V. A generic approach for the catalytic reduction of nitriles. *Tetrahedron* 2003, 59, 5417–5423.
47. Zhang Y-K; Plattner JJ; Freund YR; Easom EE; Zhou Y; Ye L; Zhou H; Waterson D; Gamo F-J; Sanz LM; Ge M; Li Z; Li L; Wang H; Cui H Benzoxaborole antimalarial agents. Part 2: Discovery of fluoro-substituted 7-(2-carboxyethyl)-1,3-dihydro-1-hydroxy-2,1-benzoxaboroles. *Bioorg. Med. Chem. Lett* 2012, 22, 1299–1307. [PubMed: 22243961]
48. Hedstrom L The dynamic determinants of reaction specificity in the IMPDH/GMPR family of (beta/alpha)(8) barrel enzymes. *Crit. Rev. Biochem. Mol. Biol* 2012, 47, 250–263. [PubMed: 22332716]
49. Franzblau SG; DeGroot MA; Cho SH; Andries K; Nuermberger E; Orme IM; Mdluli K; Angulo-Barturen I; Dick T; Dartois V; Lenaerts AJ Comprehensive analysis of methods used for the evaluation of compounds against *Mycobacterium tuberculosis*. *Tuberculosis* 2012, 92, 453–488. [PubMed: 22940006]
50. Katsuno K; Burrows JN; Duncan K; Hooft van Huijsduijnen R; Kaneko T; Kita K; Mowbray CE; Schmatz D; Warner P; Slingsby BT Hit and lead criteria in drug discovery for infectious diseases of the developing world. *Na. Rev. Drug Discov* 2015, 14, 751–8.
51. Singh V; Brecik M; Mukherjee R; Evans JC; Svetlikova Z; Blasko J; Surade S; Blackburn J; Warner DF; Mikusova K; Mizrahi V The complex mechanism of antimycobacterial action of 5-fluorouracil. *Chem. Biol* 2015, 22, 63–75. [PubMed: 25544046]
52. Abrahams GL; Kumar A; Savvi S; Hung AW; Wen S; Abell C; Barry CE, 3rd; Sherman DR; Boshoff HI; Mizrahi V Pathway-selective sensitization of *Mycobacterium tuberculosis* for target-based whole-cell screening. *Chem. Biol* 2012, 19, 844–854. [PubMed: 22840772]

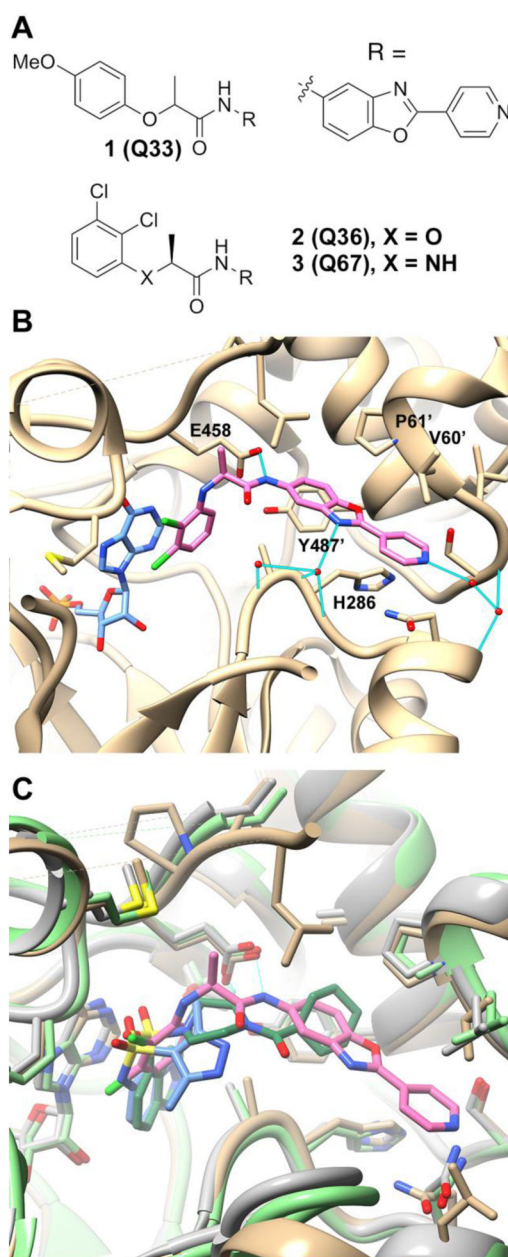


Figure 1.
Inhibitors of *Mtb*IMPDH2. **A)** Structures of **1**, **2** and **3**. **B)** Crystal structure of *Mtb*IMPDH2 CBS •IMP•**3** (PDB 4ZQO)⁹. **3** is pink, IMP is blue, hydrogen bonds are shown in cyan, residues from the adjacent subunit are marked with '. **C)** Crystal structures of *M. thermoresistible* IMPDH2 in complex with IMP and cyclohexyl[4-(5-isoquinolinylsulfonyl)-1-piperazinyl]methanone (VCC234718, PDB 5J5R, protein and IMP are spring green, inhibitor is forest green)¹¹, and N-1H-indazol-6-yl-3,5-dimethyl-1H-pyrazole-4-sulfonamide (6Q9, PDB 5K4X, protein and IMP are gray, inhibitor is blue)¹⁰. The structure of *Mtb*IMPDH2 CBS •IMP•**3** (PDB 4ZQO, protein and IMP are tan, **3** is pink)⁹ is also included. This figure was produced with UCSF Chimera⁴⁴.

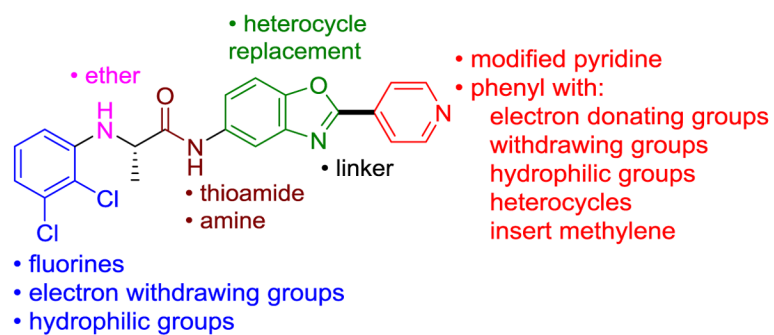


Figure 2.
An overview of the SAR explored in this study.

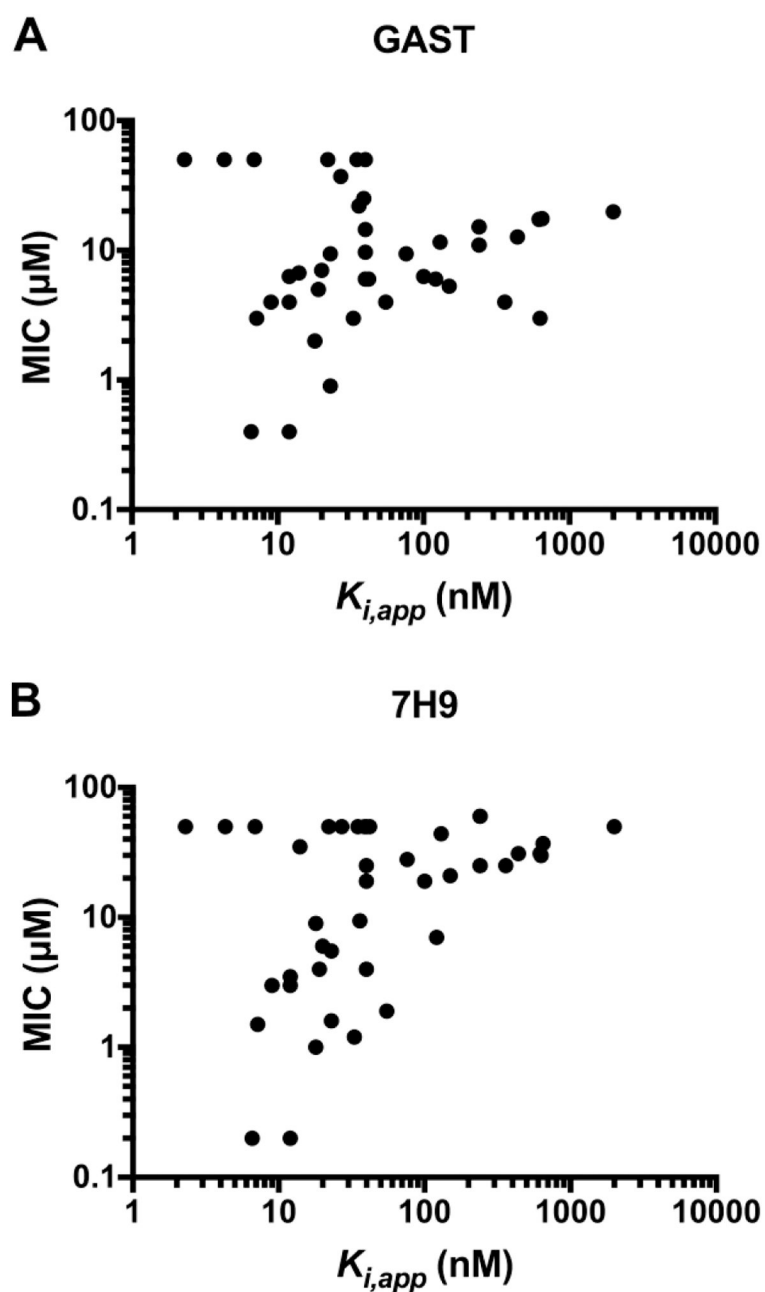


Figure 3. Correlation between antibacterial activity and enzyme inhibition for Q series compounds. Values from Table 4 and Makowska-Grzyska et al.⁹. *Mtb* H37Rv cultured in A) GAST medium and B) 7H9 medium.

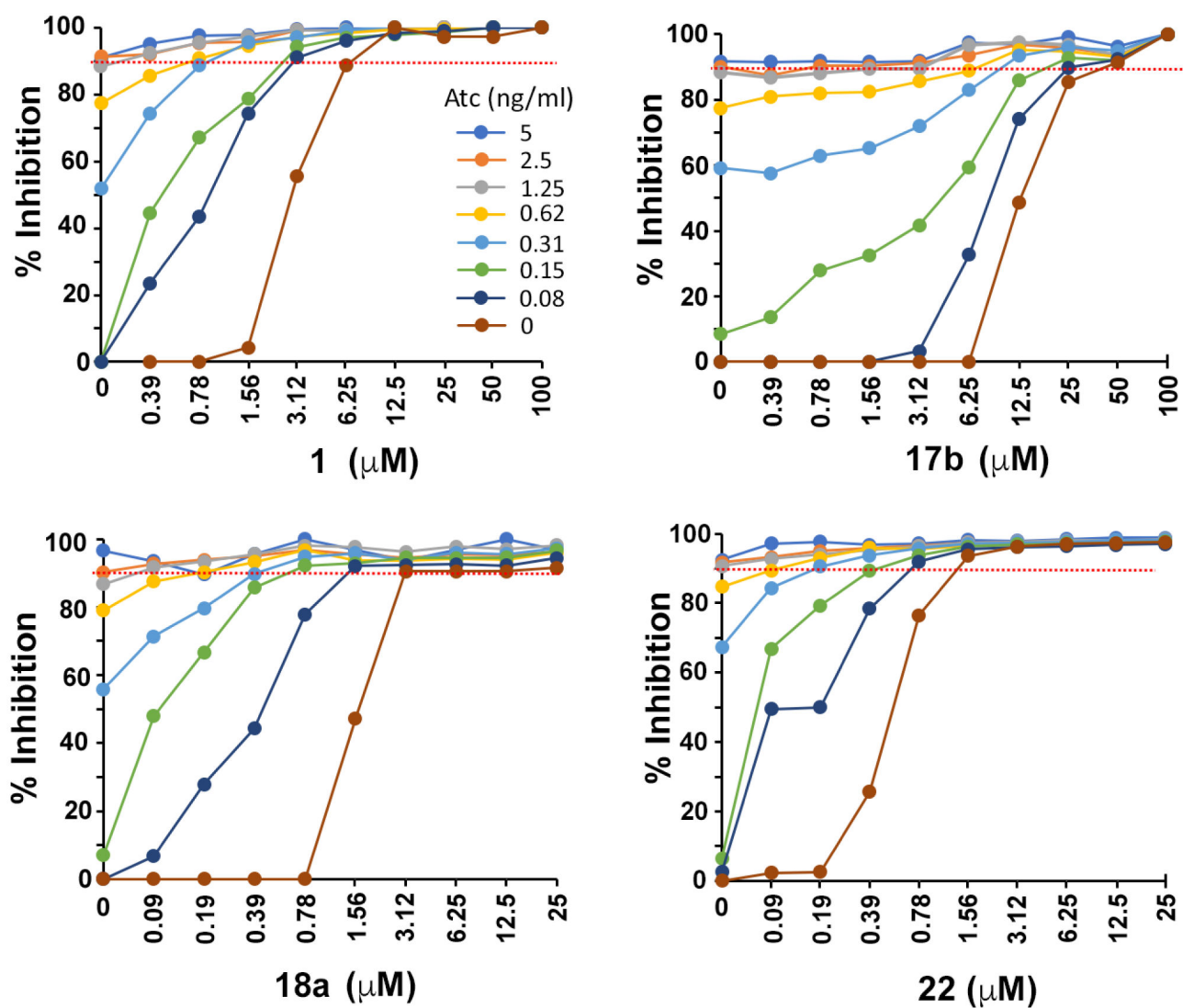


Figure 4. Knockdown of *Mtb*IMPDPH2 hypersensitizes *Mtb* to Q compounds. Regulated expression of *guaB2* is achieved in a TET-OFF system, as previously described¹¹. Addition of anhydrotetracycline (ATc) represses expression of *guaB2*, decreasing the level of *Mtb*IMPDPH2 within the bacteria. ATc concentrations (ng/mL) are 0 (dark orange), 0.08 (dark blue), 0.15 (green), 0.31 (sky blue), 0.62 (yellow), 1.25 (gray), 2.5 (orange) and 5 (royal blue).

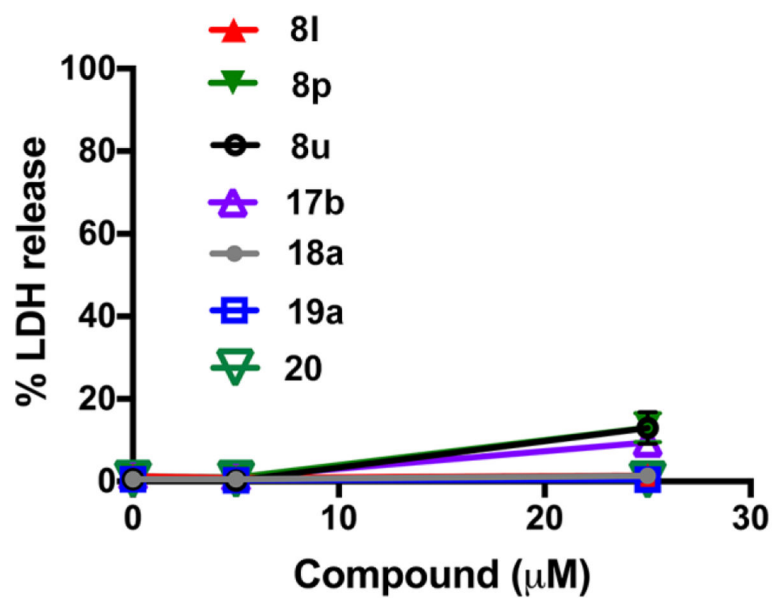
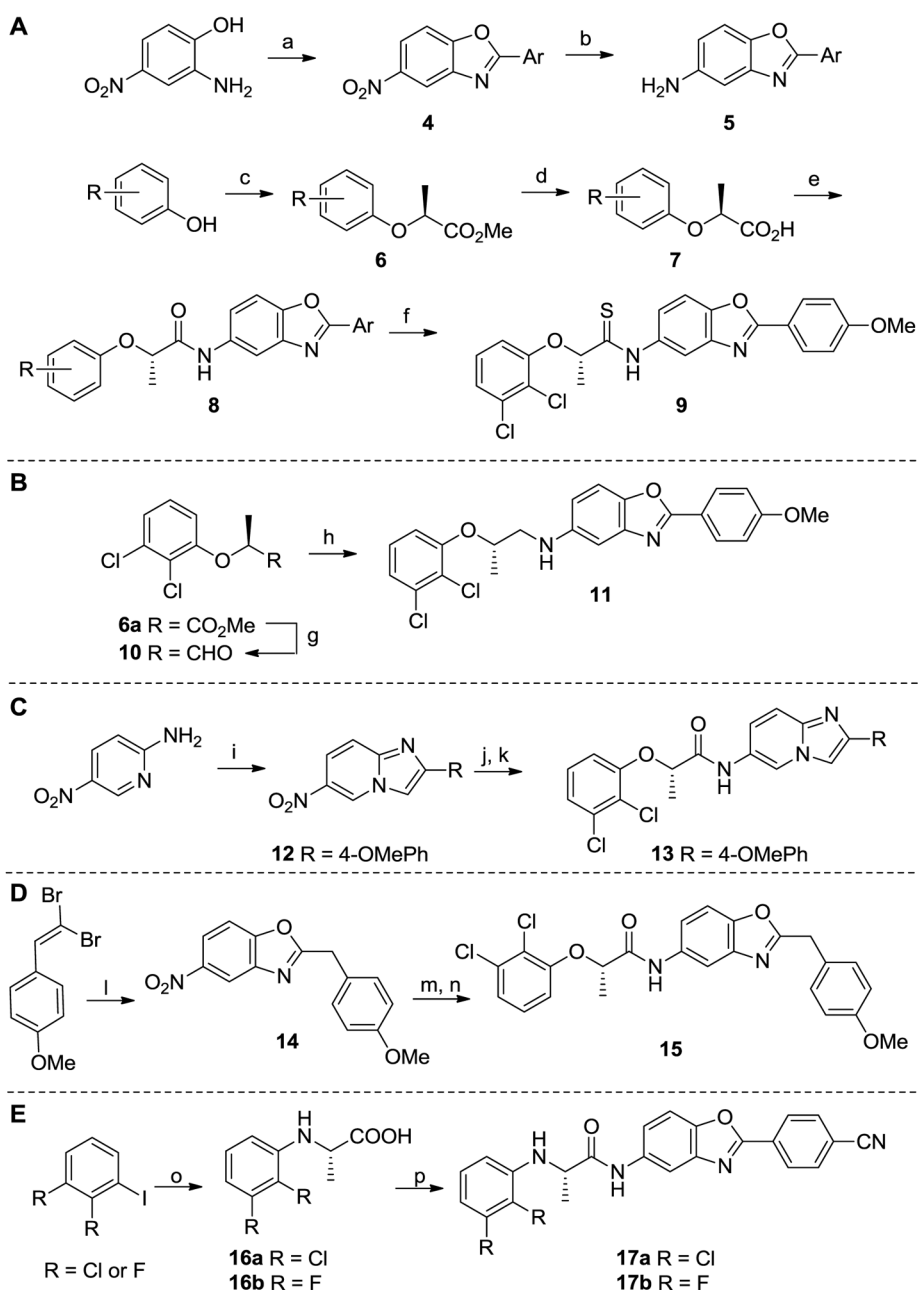


Figure 5.
Cytotoxicity of select Q compounds in HepG2 cells after 24 h.

**Scheme 1.**

Synthesis of various aryl benzoxazoles **8**, thioamide **9**, amine **11**, imidazo[1,2-a]pyridine **13**, methylene linked derivative **15** and N-arylated benzoxazoles **17a-b**.^a

^aReagents and conditions: (a) ArCHO, DarcoKB, O₂ (1 atm), xylene 140 °C, 6–8 h, 70–80%; (b) 10% Pd/C, H₂ (1 atm), EtOAc:MeOH, 3 h, 85–94%; (c) PPh₃, DEAD, (+)-methyl D-lactate, THF, 0 °C to rt, 4 h, 85–90%, (d) LiOH, THF:MeOH, 4 h, 86–91%; (e) **5**, EDC-HCl, DMF, 12 h, 62–79%. (f) Lawesson's reagent, 1,4-dioxane, reflux, 2 h, 71%; (g) **1**, DIBAL-H, DCM, –78 °C, 1h, 89%, (h) **5** (Ar = 4-OMePh), NaBH(OAc)₃, DCE, 1.5 h, 81%; (i) 4-OMePhC(O)CH₂Br, NaHCO₃, EtOH, reflux, 12 h, 88%; (j) SnCl₂, EtOH:EtOAc,

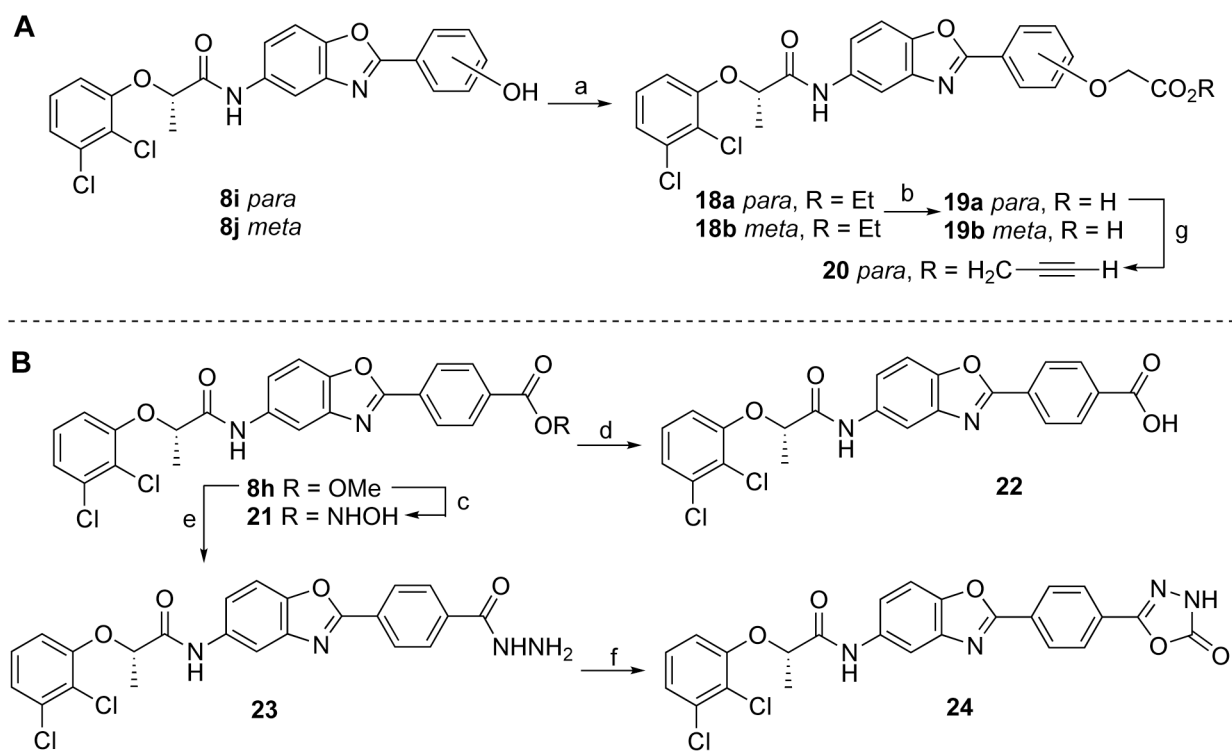
reflux, 2 h; (k) **7** (R = 2,3-diCl), EDC·HCl, DMF, rt, 12 h, 60%; (l) 2-amino-4-nitrophenol, DABCO, NMP, 100 °C, 24 h, 60%; (m) 10% Pd/C, H₂, MeOH:EtOAc, 2–3 h; (n) **7** (R = 2,3-diCl), EDC·HCl, DMF, rt, 12 h, 67%; (o) L-alanine, CuI, Cs₂CO₃, DMF, 90 °C, 24 h; (p) **5** (Ar = 4-CNPh), HATU, DMF, rt, 12 h, 45–54%.

Author Manuscript

Author Manuscript

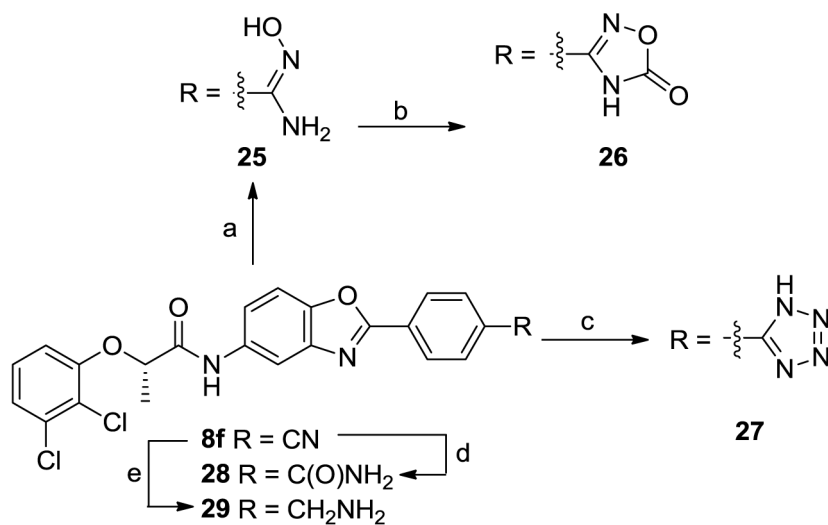
Author Manuscript

Author Manuscript

**Scheme 2.**

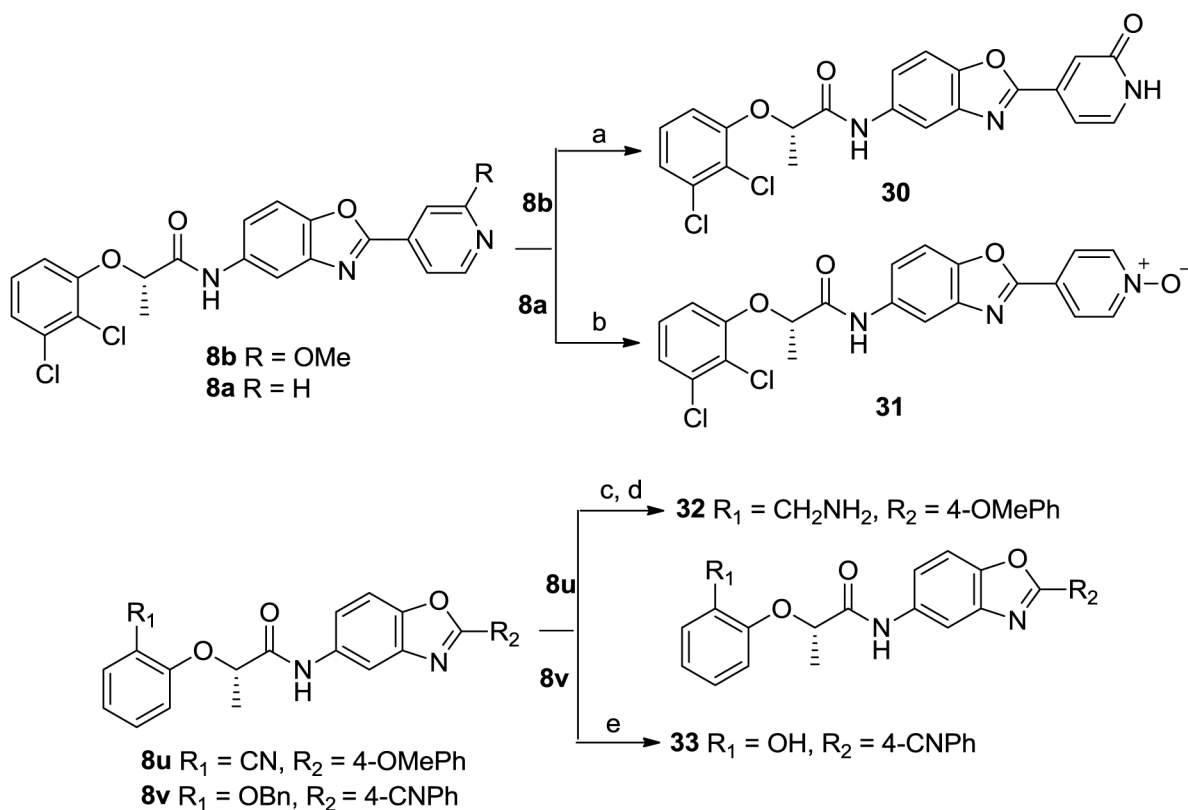
Synthesis of derivatives **18a-b**, **19a-b** and **20-24**.^a

^aReagents and conditions: (a) BrCH₂COEt, K₂CO₃, DMF, rt, 6 h, 80–83%; (b) LiOH, THF:MeOH, rt, 86–88%; (c) NH₂OH·HCl, KOH, MeOH, rt, 12 h, 65%; (d) NaOH, THF:MeOH:H₂O (3:1:1), 2 h, rt, 90%; (e) NH₂NH₂·H₂O, EtOH, reflux, 5 h, 67%; (f) CDI, DIPEA, DMF, rt, 2 h, 66%; (g) CH≡CCH₂Br, K₂CO₃, DMF, rt, 6 h, 81%.

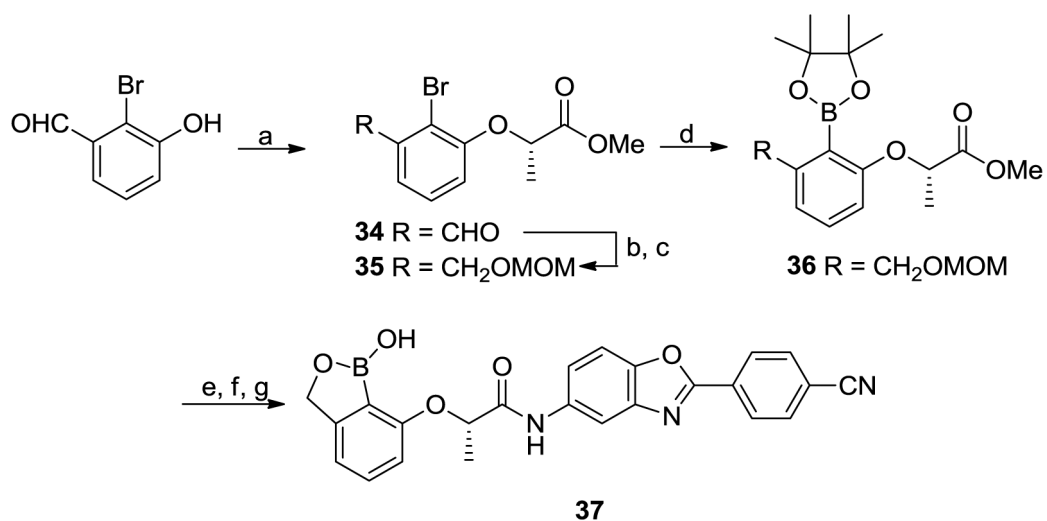
**Scheme 3.**

Synthesis of derivatives **25-29** from **8f**.^a

^aReagents and conditions: (a) $\text{NH}_2\text{OH}\cdot\text{HCl}$, Et_3N , EtOH , reflux, 4 h, 82%; (b) CDI, DIPEA, DMF, rt, 2 h, 61%; (c) NaN_3 , NH_4Cl , DMF, 100 °C, 6 h, 62%; (d) $t\text{-BuOK}$, $t\text{-BuOH}$, 12 h, 54%; (e) 1. $\text{NiCl}_2\cdot 6\text{H}_2\text{O}$, NaBH_4 , Boc_2O , $\text{MeOH}:\text{THF}$, rt, 2 h, 2. TFA, DCM, rt, 4 h, 67%.

**Scheme 4.**Synthesis of derivatives **30-33**.^a

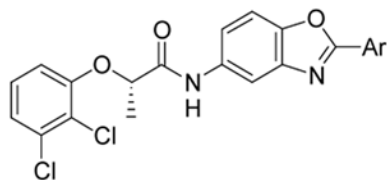
^aReagents and conditions: (a) LiCl, p-TSA, DMF, 120 °C, 2 h, 77%; (b) *m*-CPBA, DCM, rt, 12 h, 74%; (c) NiCl₂·H₂O, NaBH₄, and then Boc₂O, THF, MeOH, rt, 4 h; (d) TFA, DCM, 68%; (e) 10% Pd/C, H₂, MeOH:EtOAc, rt, 3 h, 90%.

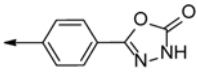
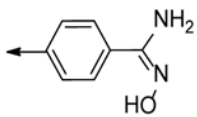
**Scheme 5.**

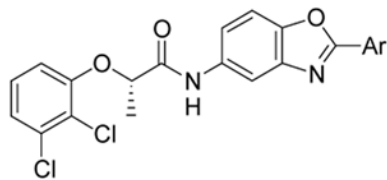
Synthesis of benzoxaborole **37**.^a

^aReagents and conditions: (a) (+)-Methyl D-lactate, DEAD, PPh₃, THF, 0 °C, 2 h, 83%; (b) NaBH₄, EtOH, rt, 1 h; (c) MOMCl, DIPEA, DCM, rt, 12 h, 72%; (d) Pin₂B₂, Pd(PPh₃)₂Cl₂, KOAc, 1,4-dioxane, 95 °C, 12 h, 64%; (e) LiOH, MeOH:THF, 4 h, 0 °C; (f) **5** (Ar = 4-CNPh), EDC·HCl, DMF, rt, 12 h; (g) 4N HCl, THF, 4 h, 28%.

Table 1.

*Mtb*IMPDH2 CBS Inhibition of Benzoxazole Derivatives Containing Various Aryl Substituents.

Cmpd	Ar	$K_{i,app}$ (nM) ^a		
		<i>Mtb</i> IMPDH2	hIMPDH2	hGMPr2
1 ^b	See Figure 1A	150 ± 50	>5000	>5000
2 (e.g. 8a) ^b	See Figure 1A	76 ± 27	>5000	>5000
3 ^b	See Figure 1A	14 ± 3	>5000	>5000
30	4-pyridin-2-one	220 ± 6	>5000	>5000
31	4-Py-N-oxide	70 ± 19	>5000	>5000
8b	4-(2-OMe)-Py	12 ± 0.1	>5000	>5000
8c	3-(6-OMe)-Py	20 ± 4	>5000	>5000
8d	4-OMe-Ph	6.9 ± 3.9	>5000	>5000
8e	4-OCF ₃ -Ph	4.3 ± 0.2	>5000	>5000
8f	4-CN-Ph	12 ± 3	2300	>5000
8g	4-F-Ph	35 ± 7	>5000	>5000
8h	4-PhCO ₂ Me	96 ± 43	>5000	>5000
8i	4-OH-Ph	50 ± 17	>5000	>5000
8j	3-OH-Ph	85 ± 30	>5000	>5000
8k	2-OH-Ph	96 ± 21	>5000	>5000
18a	4-Ph-OCH ₂ CO ₂ Et	6.6 ± 0.4	>5000	>5000
20	4-Ph-OCH ₂ CO ₂ CH ₂ CCH	12 ± 2	>5000	>5000
19a	4-Ph-OCH ₂ CO ₂ H	18 ± 3	>5000	>5000
18b	3-Ph-OCH ₂ CO ₂ Et	23 ± 1	>5000	>5000
19b	3-Ph-OCH ₂ CO ₂ H	55 ± 10	>5000	>5000
21	4-Ph-C(O)NHOH	630 ± 210	>5000	>5000
22	4-PhCO ₂ H	360 ± 140	>5000	>5000
23	4-Ph-C(O)NHNH ₂	49 ± 6	>5000	>5000
24		2.3 ± 1.0	2900	>5000
25		39 ± 12	>5000	>5000



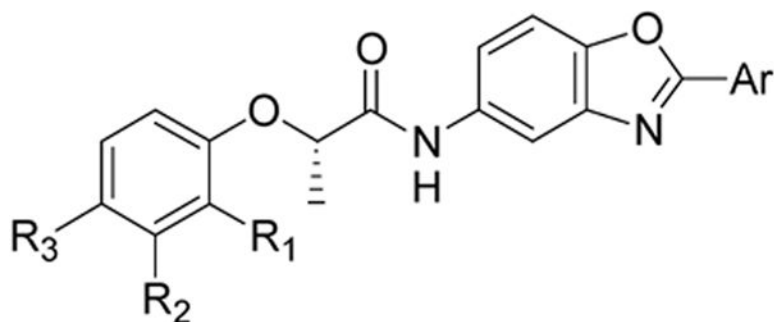
Cmpd	Ar	$K_{i,app}$ (nM) ^a		
		<i>Mtb</i> IMPDH2	hIMPDH2	hGMPR2
26		46 ± 12	>5000	>5000
27	4-Ph-tetrazole	51 ± 2	>5000	>5000
28	4-Ph-C(O)NH ₂	64 ± 26	>5000	>5000
29	4-Ph-CH ₂ NH ₂	240 ± 26	>5000	>5000

^aValues are the average and range of at least two independent determinations.

* Single determination.

^bValues from Makowska-Grzyska *et al*⁹.

Table 2.

*Mtb*IMPDH2 CBS Inhibition of Benzoxazole Derivatives Containing Various Phenyl Ether Substituents.

Cmpd	R ₁	R ₂	R ₃	Ar	$K_{i,app}^a$ (nM)		
					<i>Mtb</i> IMPDH2	hIMPDH2	hGMPR2
8l	F	F	H	4-Py	55 ± 9	>5000	>5000
8m	F	F	H	4-OMe-Ph	19 ± 2	>5000	>5000
8n	F	F	H	4-OH-Ph	121 ± 21	>5000	>5000
8o	F	F	H	3-(6-OMe)-Py	42 ± 17	>5000	>5000
8p	F	F	H	4-CN-Ph	7.2 ± 2.5	2000	>5000
8q	F	F	H	4-F-Ph	40 ± 3	>5000	>5000
8r	F	F	F	4-CN-Ph	22 ± 11	>5000	>5000
8s	CN	H	H	4-Py	76 ± 35	>5000	>5000
8t	CN	F	H	4-Py	40 ± 2	>5000	>5000
8u	CN	H	H	4-OMePh	33 ± 5	>5000	>5000
8v	OBn	H	H	4-CN-Ph	43 ± 12	>5000	>5000
32	CH ₂ NH ₂	H	H	4-OMe-Ph	23 ± 9	>5000	>5000
33	OH	H	H	4-CN-Ph	36 ± 12	>5000	>5000
37	B(OH)OCH ₂	H		4-CN-Ph	370 ± 70 *	>5000	>5000

^a Values are the average and range of at least two independent determinations.

* Single determination, error of the fit is listed.

Table 3.*Mtb*IMPDPH2 CBS Inhibition of Other Benzoxazole Derivatives.

Cmpd	Structure	$K_{i,app}^a$ (nM)		
		<i>Mtb</i> IMPDPH2	hIMPDPH2	hGMPPR2
9		27 ± 21	>5000	>5000
11		1290 ± 250 [*]	n.a.	>5000
13		160 ± 4	>5000	>5000
15		100 ± 40	>5000	>5000
17a		9 ± 4	3300	>5000
17b		18 ± 3	>5000	>5000

^a Values are the average and range of at least two independent determinations.^{*} Single determination.

Table 4.

Antitubercular activity of *Mtb*IMPDPH2 inhibitors against *Mtb* H37Rv. The number of independent determinations is shown in parentheses.

Compound	GAST/Fe MIC (μ M) ^a		7H9/ADC/Tween MIC (μ M) ^a	
	-Gua	+Gua	-Gua	+Gua
1 ^b	5.3 \pm 0.9 (3)	24 \pm 16 (3)	10 \pm 2 (3)	21 \pm 4 (3)
2 (e.g. 8a) ^b	9.4 \pm 3.0 (2)	37 (1)	16 \pm 6 (3)	28 \pm 9 (2)
3 ^b	6.7 \pm 3 (2)	50 (1)	12 \pm 6 (3)	35 \pm 15 (2)
8b	6.3 \pm 0.0 (2)	6.3 \pm 0.0 (2)	3.5 \pm 1.2 (2)	14 \pm 5 (2)
8c	7 \pm 2 (3)	9 \pm 7 (3)	6 \pm 3 (3)	> 25 (3)
8d	>50 (2)	>50 (2)	>50 (2)	>50 (2)
8e	>50 (1)	>50 (1)	>50 (2)	>50 (2)
8f	4 \pm 1 (3)	5 \pm 1 (3)	3 \pm 1 (4)	6 \pm 1 (4)
8g	>50 (2)	>50 (2)	>50 (2)	>50 (2)
8l	4 \pm 2 (2)	6.3 \pm 0 (2)	1.9 \pm 0.5 (2)	4 \pm 3 (2)
8m	5 \pm 2 (3)	8 \pm 4 (3)	4 \pm 4 (4)	14 \pm 7 (4)
8n	6 (1)	19 (1)	7 \pm 3 (2)	>30 (2)
8o	6 \pm 5 (2)	8 \pm 7 (2)	>50 (5)	>50 (5)
8p	3 \pm 1 (3)	6.3 \pm 0 (2)	1.5 \pm 0.8 (6)	4 \pm 3 (6)
8q	>50 (1)	>50 (2)	>50 (2)	>50 (2)
8r	>50 (2)	>50 (2)	>50 (5)	>50 (5)
8t	6 \pm 4 (2)	11 \pm 2 (2)	4 \pm 1 (2)	8 \pm 2 (2)
8u	3.1 \pm 0.0 (2)	6.3 \pm 0.0 (2)	1.2 \pm 0.0 (2)	4.7 \pm 0.0 (2)
9	37 (1)	>50 (1)	>50 (2)	>50 (2)
17a	4 \pm 3 (2)	13 \pm 9 (2)	3 \pm 1 (2)	6 \pm 1 (2)
17b	2 \pm 1 (2)	6 \pm 0 (2)	1.0 \pm 0.3 (2)	1.4 \pm 0.3 (2)
18a	0.4 \pm 0.0 (2)	0.5 \pm 0.1 (2)	0.2 \pm 0.1 (2)	0.23 \pm 0.16 (2)

Compound	GAST/Fe MIC (μM) ^a		7H9/ADC/Tween MIC (μM) ^a	
	-Gua	+Gua	-Gua	+Gua
18b	0.9 \pm 0.2 (2)	1.4 \pm 0.2 (2)	1.6 \pm 0.0 (2)	1.6 \pm 0.0 (2)
19a	2 \pm 1 (4)	4 \pm 2 (4)	9 \pm 4 (5)	20 \pm 10 (5)
20	0.4 \pm 0.0 (2)	1.4 \pm 0.2 (2)	0.2 \pm 0 (2)	0.4 \pm 0 (2)
21	3 \pm 1 (4)	6 \pm 1 (4)	30 \pm 10 (5)	>50 (5)
22	4 \pm 2 (2)	5 \pm 0 (2)	>25 (2)	>50 (2)
24	>50 (2)	>50 (2)	>50 (2)	>50 (2)
25	25 (1)	25 (1)	>50 (2)	>50 (2)
29	11 \pm 2 (2)	11 \pm 2 (2)	25 \pm 12 (2)	25 \pm 12 (2)
32	9.4 \pm 3.1 (2)	16 \pm 3 (2)	5.5 \pm 0.8 (2)	9.4 \pm 0.0 (2)
33	22 \pm 3 (2)	25 \pm 0.0 (2)	9.4 \pm 0.0 (2)	22 \pm 3 (2)

^aMICs determined after 1 week in culture.

^bValues from Makowska-Grzyska et al⁹. +Gua, 200 μM guanine.

Table 5.

Antibacterial activity against SRMV2.6. H37Rv is the wild-type strain. b. SRMV2.6 contains *Mtb*IMPDH2/Y487C, which confers resistance to the isoquinoline sulfonamide inhibitor VCC234718¹¹.

Compound	WT ^a <i>K</i> _{i,app} (nM)	Y487C ^b <i>K</i> _{i,app} (μM)	Ratio <i>K</i> _{i,app} (Y487C) / <i>K</i> _{i,app} (WT)	MIC (μM) ^c		
				H37Rv	H37Rv (+ATc)	SRMV2.6
1	150 ± 50	>50 ^d	>300	12.5	12.5	>100
17b	18 ± 3	1.1 ± 0.1	60	3.1	3.1	>100
18a	6.6 ± 0.4	~13 ^f	~2000	3.1	3.1	3.1
22	360 ± 140	>15 ^e	>40	25	25	25

^a. Inhibition of purified wild-type *Mtb*IMPDH2.

^b. Inhibition of purified *Mtb*IMPDH2/Y487C

^c. Bacteria were cultured in 7H9/Glycerol/OADC/Tween and growth was measured with Alamar Blue as previously described¹¹, +ATc, 100 ng/mL.

^d. 20% inhibition at 50 μM.

^e. 5-10% inhibition at 15 μM.

^f. 80% inhibition at 50 μM.